

Systematic revision of the Cambrian trilobite *Bathynotus* Hall, 1860, with documentation of new occurrences in western Laurentia and implications for intercontinental biostratigraphic correlation

MARK WEBSTER

WEBSTER, M. 2009:12:24. Systematic revision of the Cambrian trilobite *Bathynotus* Hall, 1860, with documentation of new occurrences in western Laurentia and implications for intercontinental biostratigraphic correlation. *Memoirs of the Association of Australasian Palaeontologists* 37, 369-406. ISSN 0810-8889.

Bathynotus is a rare trilobite genus known from the Cambrian Stage 4 to Stage 5 boundary interval of Laurentia, South China, Australia and Siberia. With its near global distribution, *Bathynotus* may prove instrumental in the resolution of intercontinental biostratigraphic correlation at this time. However, this potential has been hampered by problems of species differentiation, which has led to uncertainty regarding the number of species within the genus and, concomitantly, the geographic and stratigraphic ranges of those species. To resolve this issue, morphometric data extracted from almost 100 specimens, including representatives of all nine purported species, were subject to multivariate and bivariate analyses. These analyses recognise a total of just four species, each diagnosable by a unique combination of character states. Systematic revisions, including amended geographic and stratigraphic ranges, are provided for *B. holopygus* (known from eastern Laurentia and South China), *B. granulatus* (including its junior synonym *B. elongatus*; known from the Siberian Altay-Sayan foldbelt, South China, and western Laurentia), *B. kueichouensis* (known from South China and Australia) and *B. namanensis* (known from the Siberian Platform). Many isolated sclerites, including the type suites of many purported species described from Siberia, are consistent with the diagnoses of more than one of the four species. Thus, isolated cranidia from western Laurentia and from Siberia may represent *B. holopygus* and/or *B. kueichouensis*, or perhaps different but currently undiagnosable species. The implications of these revisions for intercontinental biostratigraphic correlation are discussed. New occurrences of *Bathynotus* in western Laurentia (Combined Metals Member, Pioche Formation, Nevada, U.S.A.) are documented.

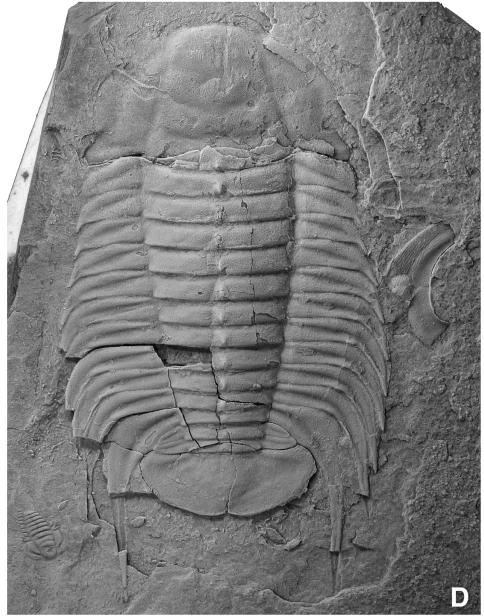
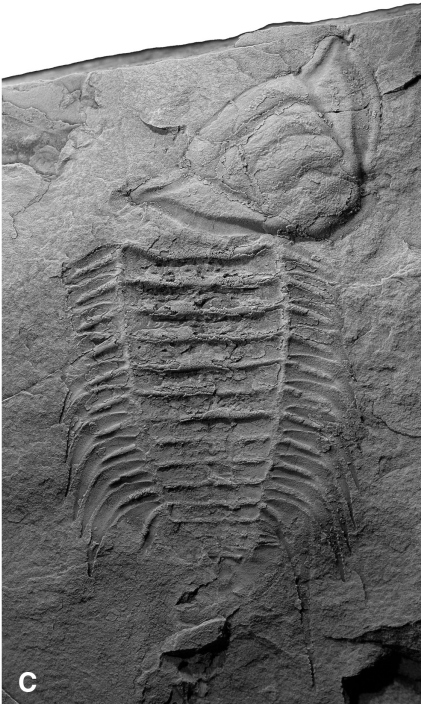
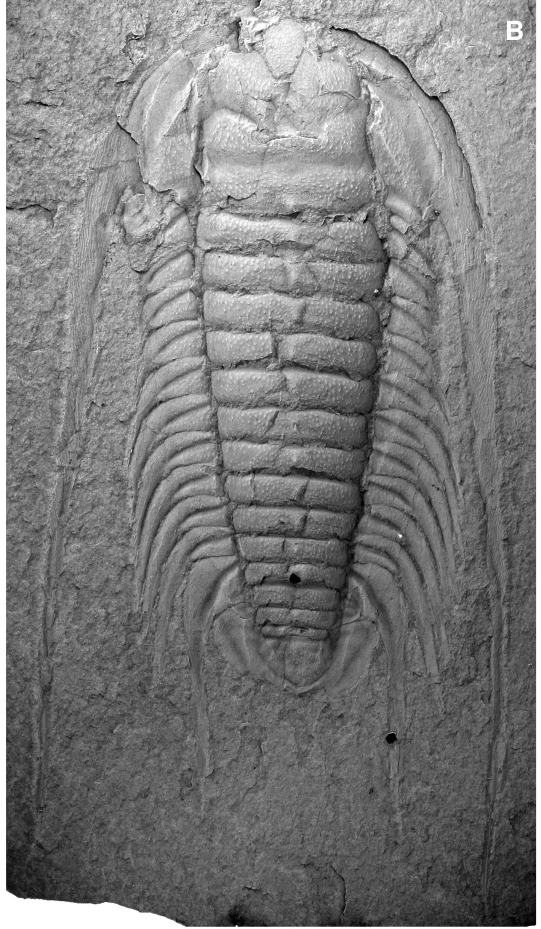
Mark Webster (mwebster@geosci.uchicago.edu), Department of the Geophysical Sciences, University of Chicago, 5734 South Ellis Avenue, Chicago, IL 60637, U.S.A. Received 28 August 2009.

Keywords: *Bathynotus*, trilobites, Cambrian, morphometrics, ontogeny, biostratigraphy.

BATHYNOTUS Hall, 1860 is a widely distributed Cambrian trilobite genus known from open shelf, outer shelf, shelf-edge, and slope deposits of Laurentia, South China, Australia and Siberia. All definitive occurrences of *Bathynotus* are within a relatively narrow stratigraphic interval, likely falling within Stages 4 and 5 of the revised international subdivisions of the Cambrian (although those stages are yet to be ratified; Peng & Babcock 2008) and often closely associated with the first appearance datum of *Oryctocephalus indicus* (Reed, 1910). *Bathynotus* in general, and the type species *B. holopygus* (Hall, 1859a) in particular, have been considered potentially

useful taxa in the ongoing effort towards refining intercontinental biostratigraphic correlation (e.g., Palmer 1998b; Sundberg *et al.* 1999; Geyer & Landing 2001; Hughes *et al.* 2002; Fletcher 2007; McCollum & Sundberg 2007; Peng & Babcock 2008; Peng *et al.* 2009).

However, *Bathynotus* is typically rare in terms of the number of localities on each palaeocontinent from which it has been recovered and of the number of specimens recovered from those localities (see Whittington [1998] for other examples of rare but widespread Cambrian trilobites). This dearth of material has limited our understanding of the range of intraspecific



morphological variation, which in turn has led to debate regarding the number, stratigraphic ranges and geographic ranges of *Bathynotus* species globally. For example, estimates of the number of species occurring in Laurentia, Australia and South China range from six (following Zhao *et al.* 1990; Öpik 1975) to one (*B. holopygus*; following Shergold & Whittington 2000), with a most recent claim of three (following Yuan *et al.* 2002; Peng *et al.* 2009). Six other species described from Siberia are known from such limited and often scrappy material that their taxonomic validity has been difficult to determine (e.g., Shergold & Whittington 2000, p. 7).

This paper presents a morphometric study of *Bathynotus* specimens from around the world, which permits quantitative analysis of intra- and interspecific variation and assessment of the degree of morphological distinction between purported taxa. Based on the result of this analysis, species-level systematics within the genus is revised: species descriptions, stratigraphic ranges and geographic ranges are amended accordingly. Occurrences of the genus in western Laurentia (Nevada, U.S.A.) are documented in detail for the first time, including the first known silicified *Bathynotus* sclerites. The implications of the revised taxonomy for global biostratigraphic correlation are discussed.

TERMINOLOGY AND SPECIES CONCEPT

Morphological terminology follows that of Whittington & Kelly (in Whittington *et al.* 1997), with the following modifications. Following Webster (2007b), genal spine advancement is measured by finding the point at which the axial furrow of the glabella is intersected by a transverse line between the genal spine bases (i.e., the adaxial margins of the genal spine bases where they contact the posterolateral cephalic margin). The qualitative location of this point of intersection relative to the contact of glabellar lobes and furrows with the axial furrow is expressed in the species descriptions. Following Palmer (1998a), thoracic segments are identified as T1 (most anterior) to Tn (most posterior). Also following Palmer (1998a), the length of a thoracic pleural spine is described as *sentate* (if the spine length is less than half of the transverse width of the inner pleural region) or *falcate* (if the spine

length is more than half of the transverse width of the inner pleural region), and a thoracic segment is described as *macropleural* if the inner pleural region markedly widens (exsag.) distally relative to the inner pleural region of adjacent segments without distorting the shape of more anterior segments. A thoracic segment is described as *macrospinous* if the pleural spine is markedly longer than those of adjacent segments. Spine length (genal or pleural) is measured from the adaxial margin of the spine base to the spine tip.

A species is here defined as the least inclusive aggregation of comparable individuals (semaphoronts) diagnosable by a unique combination of character states. Such a pattern-based definition identifies species boundaries based on available morphological data. Species delimitation is therefore regarded as a testable hypothesis amenable to falsification in the face of additional data. This definition essentially follows the phylogenetic species concept (PSC; Nixon & Wheeler 1990; Wheeler & Platnick in Wheeler & Meier 2000). The PSC and/or the slightly modified version followed herein has been explicitly or implicitly employed by others (e.g., Cheetham 1986; Jackson & Cheetham 1990, 1994; Budd & Coates 1992; Hughes 1994; Webster 2007a, b; Webster 2009; Hopkins & Webster 2009; see also summaries by Smith 1994; Wheeler & Platnick in Wheeler & Meier 2000; Foote & Miller 2007; Hall & Hallgrímsson 2008) and offers the most testable and defensible approach to species recognition in the fossil record.

OCCURRENCES AND CURRENT TAXONOMY OF *BATHYNOTUS*

Eastern Laurentia: Vermont

Bathynotus holopygus (Fig. 1A, B), type species of the genus, has been recorded from several localities in the Parker Formation (= Parker Shale, Parker Slate) of northwestern Vermont (Shaw 1954; see systematic palaeontology section below). All occurrences are late Dyeran (traditional "Lower Cambrian" of Laurentia; Palmer 1998c) in age.

The Parker Formation is interpreted to have been deposited in a persistently dysoxic/anoxic upper slope environment in the Franklin Basin (Shaw 1958; Landing 2007, p. 48). Trilobites from the Gorge and Highgate Formations

Fig. 1. Articulated specimens of *Bathynotus*. **A-B**, *Bathynotus holopygus* (Hall, 1859a) from the Parker Formation, USNM locality 319m, Parker's Quarry, Franklin County, northwestern Vermont. **A**, Plastoholotype, FMNH UC13273, x1.5. **B**, Latex replica of USNM 15409 (2550), x2. **C**, *Bathynotus granulatus* Lermontova, 1940 from the Combined Metals Member of Pioche Formation, ICS-10255, Oak Spring Summit, Lincoln County, Nevada, FMNH PE58120, x1.5. **D**, *Bathynotus kweichouensis* Lu in Wang, 1964 from the Kaili Formation, Wuliu-Zhengjian section, Balang, Guizhou Province, South China, FMNH PE58139, x1.75.

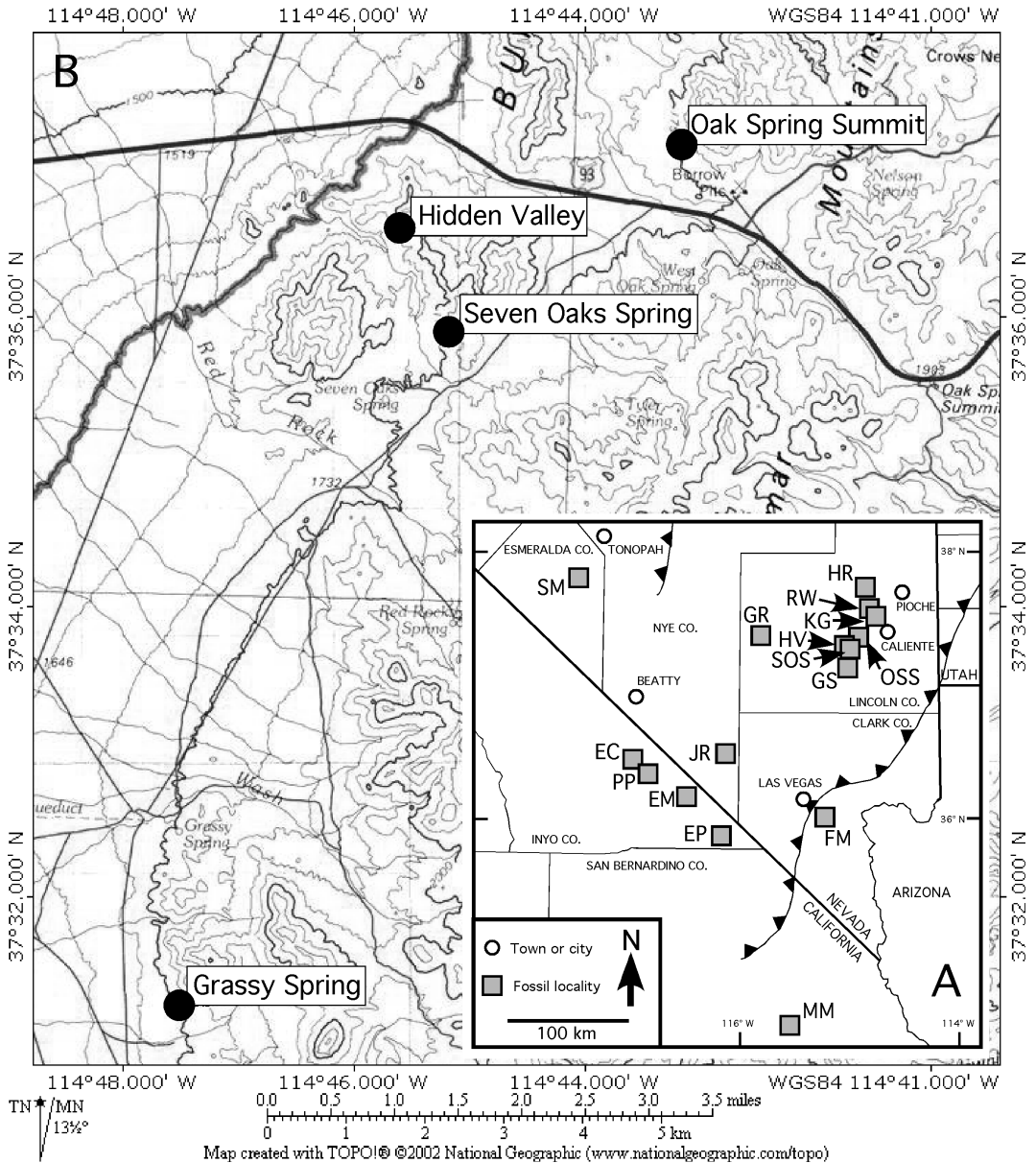


Fig. 2. A, Regional map of southern Nevada and southeastern California, U.S.A., showing localities at which the Dyeran-Delamaran boundary interval has been studied in detail by the present author. Occurrences of *Bathynotus* are restricted to the four localities just southwest of Caliente, Lincoln County, Nevada. Abbreviations: EC, Echo Canyon, Funeral Mountains; EM, Eagle Mountain; EP, Emigrant Pass section, Nopah Range; FM, Frenchman Mountain; GR, Groom Range; GS, Grassy Spring section, Delamar Mountains (Fig. 12, Appendix 2); HR, Highland Range (several sections); HV, Hidden Valley section, Burnt Springs Range (Fig. 10, Appendix 2); JR, Jaybird Ridge section, Spring Mountains; KG, Klondike Gap section, Chief Range (Webster *et al.* 2003); MM, Marble Mountains (Webster *et al.* 2003); OSS, Oak Spring Summit section, Delamar Mountains (Fig. 9, Appendix 2); PP, Pyramid Peak section, Funeral Mountains; RW, Ruin Wash section, Chief Range (Webster *et al.* 2008); SM, Split Mountain; SOS, Seven Oaks Spring section, Burnt Springs Range (Fig. 11, Appendix 2). Black lines with triangles mark eastern limits of thrusting (Antler Orogenic Belt in N, Sevier Orogenic Belt in SE; overthrust block to W in each case). B, Local topographic map of a portion of southern Lincoln County, Nevada, showing location of measured sections from which *Bathynotus* specimens have been recovered (Appendix 2). Local map created with TOPO! software (© National Geographic, 2002).

(Millardan to Ibexian) in the Franklin Basin have been interpreted as allochthonous, sourced from the carbonate platform of the Middlebury synclinorium to the south (Landing 1983, 2007, p. 48). However, many specimens of *B. holopygus* from Parker's Cobble are interpreted as moult (Whittington 1988, p. 584), which is inconsistent with the sclerites having been transported to the site (Fortey 1975; Speyer & Brett 1985; Brett & Baird 1986, 1993; Speyer 1987; Mikulic 1990; Brett & Allison 1998; Gaines & Droser 2003; Brett *et al.* 2006; Paterson *et al.* 2007; Webster *et al.* 2008). The Franklin Basin environment was likely to have been at least occasionally favourable for habitation by trilobites during deposition of the upper Dyeran Parker Formation.

Five *Bathynotus* specimens (including the plastoholotype of *B. holopygus*) from Vermont were included in the morphometric analysis (Appendix 1).

Northeastern Laurentia: Scotland?

Peach (1894, p. 671; Peach *et al.* 1907; Morris 1988) tentatively assigned several cephalic fragments collected from the Fucoid Beds (An t'Srón Formation) of Meall a'Ghubhais in the Northwest Highlands of Scotland to "*Bathynotus holopygia*" [sic], potentially representing a northeastern Laurentian occurrence of the species. However, the material was not figured, and has not been re-examined as part of the present study (and may now be lost: P. Shepherd and M. Dean, pers. comm. 2009). The collection is likely middle Dyeran in age (Palmer & Repina 1993), and represents an anomalously low stratigraphic occurrence of *Bathynotus* if the identification is accurate. Pending re-examination or collection of new material, this occurrence of the species (and genus) must be considered highly questionable (see also note in Cowie *et al.* 1972, p. 28).

Western Laurentia: Nevada

Intensive fieldwork over the last 17 years associated with refining the upper Dyeran and basal Delamaran (traditional "Middle Cambrian" of Laurentia; Palmer 1998a, c) biostratigraphy of western Laurentia (Sundberg & McCollum 1997, 2000, 2003a, b; Palmer 1998a, c; Eddy & McCollum 1998; Sundberg *et al.* 1999; Webster 2003, 2005, 2007a, b; McCollum & Sundberg 2007) has yielded 15 *Bathynotus* specimens from four localities in Nevada (Fig. 2; Appendix 2). Palmer (1998a, fig. 4) identified the then-available specimen (a single cranidium; Fig. 3E, F) as *B. holopygus* and noted the occurrence at approximately two metres below the top of the Dyeran in a biostratigraphic range chart. This occurrence was subsequently mentioned by

other workers (Sundberg *et al.* 1999; Shergold & Whittington 2000; Sundberg & McCollum 2000, fig. 2 [shown as three metres below the base of the Delamaran]; Peng *et al.* 2009). However, beyond this initial note the western Laurentian material has remained unstudied and unfigured. Based on the now-available material, all occurrences are in the uppermost 4.9 metres of the Combined Metals Member of the Pioche Formation (Appendix 2). The lithostratigraphic subdivision of the Pioche Formation used here follows Sundberg & McCollum (2000); the *Bathynotus*-bearing strata fall within the informal C-shale member of previous workers (Merriam 1964; Palmer 1998a). The *Bathynotus* specimens co-occur with the olenelloids *Nephrolenellus geniculatus* Palmer, 1998a, *Olenellus chiefensis* Palmer, 1998a, *O. fowleri* Palmer, 1998a, *O. gilberti* Meek in White, 1874, *O. terminatus* Palmer, 1998a, and *Bolbolenellus brevispinus* Palmer, 1998a, plus the oryctocephalid *Oryctocephalites palmeri* (Sundberg & McCollum 1997) and the zacanthoidid *Zacanthopsis palmeri* Hopkins & Webster, 2009 (Appendix 2). This assemblage is characteristic of the upper part (*N. geniculatus* Subzone) of the *Nephrolenellus multinodus* Zone in the high-resolution biostratigraphic scheme for the Dyeran of western Laurentia currently in development (Webster 2003; see also Webster 2007a); this is the highest zone recognised in the Dyeran. *Nephrolenellus multinodus* (Palmer in Palmer & Halley, 1979), defining the lower part of the *N. multinodus* Zone, is found just below the *Bathynotus* occurrences at all four localities (Appendix 2). The ribbon limestone at the base of the overlying Comet Shale Member contains the ptychoparioid "*Eokochaspis*" *nodosa* Sundberg & McCollum, 2000 that defines the base of the Delamaran Stage (Palmer 1998a, c; Sundberg & McCollum 2000). This limestone rests directly on top of the olenelloid-bearing Dyeran shale. Both the shale and the ribbon limestone have been interpreted as having been deposited in relatively deep water (see below), and the succession appears conformable (see also Palmer 1998a). However, some southern Great Basin sections record a shallowing event at or just below the base of the Delamaran with a subsequent deepening in the earliest Delamaran (McCollum & McCollum 1994), and it has been suggested that the shale-carbonate contact in this region is in fact a cryptic unconformity. Nevertheless, none of the high-resolution Dyeran trilobite zones (Webster 2003) are missing from the section and the temporal magnitude of any such unconformity would be small.

The uppermost Combined Metals Member of the Pioche Formation is interpreted as having

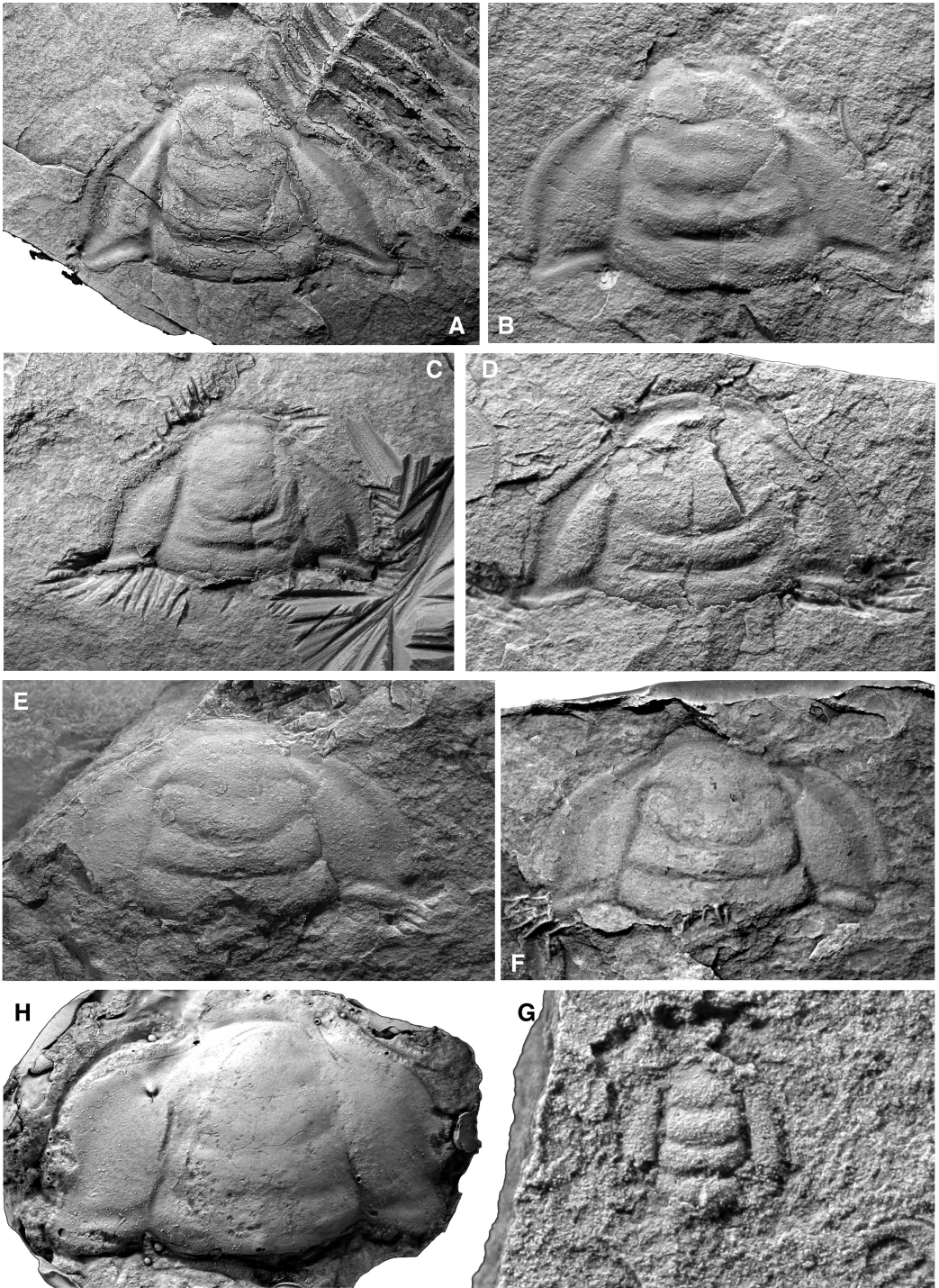


Fig. 3. Cranidia of *Bathynotus granulatus* Lermontova, 1940 (**A**, **G**), *Bathynotus namanensis* Lermontova, 1940 (**H**) and *Bathynotus* sp. indet. (**B**-**F**). **A**, Cranidium of specimen in Fig. 1C, internal mould, FMNH PE58120, from ICS-10255, x2. **B**, internal mould, FMNH PE58127, from ICS-1178, x3. **C**, internal mould, FMNH PE58131, from ICS-1163, x3. **D**, internal mould, FMNH PE58128, from ICS-1186, x4. **E**, **F**, internal mould and latex cast of external mould of FMNH PE58126, from ICS-1024, x3. **G**, morphologically immature cranidium, internal mould, FMNH PE58132, from ICS-1163, x10. **H**, latex replica of lectotype of *B. namanensis*, (continued opposite)

been deposited on the floor of a broad shelf sea covering what is now the southern Great Basin (Palmer & Halley 1979; Palmer 1998a; Sundberg & McCollum 2000). Throughout much of the late Dyeran a carbonate belt was developed on the shelf (represented by the Mule Spring Limestone of western Nevada and eastern California; inboard extensions of which are represented by the cliff-forming lower portion of the Combined Metals Member in eastern Nevada and by the Gold Ace Limestone Member of the Carrara Formation and the Chambless Limestone in south-central Nevada and southeastern California). This carbonate belt apparently served as a barrier, limiting incursions of outer shelf and shelf-edge taxa onto the inner shelf. However, a substantial relative transgression and highstand in the latest Dyeran (*Nephrolenellus multinodus* Zone) drowned the carbonate belt (Webster *et al.* 2008), so that siliciclastic deposition spread across the entire shelf just prior to the Dyeran-Delamaran boundary (represented by the Emigrant Formation, the Cadiz Formation, the basal Pyramid Shale Member of the Carrara Formation, and the upper portion of the Combined Metals Member south of the northern Highland Range; McCollum & McCollum 1994; McCollum & Sundberg 1999; Sundberg & McCollum 2003a, b; Webster *et al.* 2008). Absence of the carbonate belt barrier in conjunction with the relative sea level rise may explain the occurrence of outer shelf trilobites such as *Bathynotus* and oryctocephalids in the uppermost Combined Metals Member, which was deposited well inboard of the shelf edge. The depositional environment of the uppermost Combined Metals Member at the Ruin Wash Lagerstätte (Palmer 1998a; Lieberman 2003; Webster *et al.* 2008), coeval with and located just 24 kilometres (15 miles) northeast of the *Bathynotus*-bearing strata of Oak Spring Summit, has been interpreted as having been below storm wave base in moderately deep water (perhaps 20 to 100 metres; Webster *et al.* 2008). A similar setting is inferred for the *Bathynotus*-bearing interval at the four localities discussed here (Fig. 2, Appendix 2).

Twelve *Bathynotus* specimens from Nevada were appropriate for inclusion in the morphometric analysis (Figs 3A-G, 4; Appendix 1).

South China

Bathynotus holopygus has been identified in South China from the lower part (*Ovatoryctocara granulata*-*Bathynotus holopygus* Zone) of the

Kaili Formation in northwestern Danzhai County, southeastern Guizhou Province (Zhao *et al.* 1990; Yuan *et al.* 2001, 2002; Peng *et al.* 2009). Twelve South China specimens figured in the literature as *B. holopygus* were appropriate for inclusion in the morphometric analysis (Appendix 1).

A similar species, *B. kueichouensis* Lu in Wang, 1964 (Fig. 1D; including junior synonyms *B. nanjiangensis* Zhang, 1981, *B. gaotanensis* Zhang & Li, 1984, *B. hunanensis* Liu, 1982, and *B. hubeiensis* Sun, 1982, following Yuan *et al.* 2002 and Peng *et al.* 2009), has been reported from the lower portion of the Kaili Formation at sections in Guizhou Province, Hunan Province, Hubei Province, and Anhui Province in South China, and from Xinjiang in northwest China (Yuan *et al.* 2002; Peng *et al.* 2009). This species was considered synonymous with *B. holopygus* by Shergold & Whittington (2000), but considered distinct by Yuan *et al.* (2002; also Wang *et al.* 2007; Peng *et al.* 2009). Peng *et al.* (2009, pp. 101-102) stated that morphologically mature *B. kueichouensis* differs from *B. holopygus* by having a wide, conical glabella that is shorter than the basal width; narrow, subtriangular fixigenae; curved and round palpebral lobes; short genal spines with posterior tips developed opposite the axial ring of T4; a wide pygidial margin; and a broad, subtriangular terminal piece on the pygidial axis. Twenty specimens figured in the literature as *B. kueichouensis* were appropriate for inclusion in the morphometric analysis (Appendix 1).

A third species of *Bathynotus*, *B. elongatus* Zhao *et al.*, 1987, has also been described from the Kaili Formation in Guizhou Province. This species was also considered synonymous with *B. holopygus* by Shergold & Whittington (2000) but was treated as a distinct taxon by Yuan *et al.* (2002; also Peng *et al.* 2009). Peng *et al.* (2009) characterised *B. elongatus* as having an elongate exoskeleton; genal spines extending almost half the body length in meraspid; narrow fixigena; palpebral lobes close to the axial furrow; a distinct terminal axial ring on the pygidium; a flat pygidial pleural field; and a (p. 102) “pygidial margin that is not developed”. Ten specimens figured in the literature as *B. elongatus* (including the holotype) were appropriate for inclusion in the morphometric analysis (Appendix 1). An image of an additional specimen posted on the internet (see Appendix 1) also provided useful morphological information for the species, but was not included in the morphometric analysis.

Unpublished photographs of twelve *Bathynotus*

specimen number 153/5156, from Namana River, Siberian Platform (see Lermontova 1940, pl. 40, fig. 1; Lermontova 1951, pl. 16, fig. 5; Lazarenko 1958, pl. 1, fig. 4). A-G from the Combined Metals Member, Pioche Formation, Lincoln County, Nevada (see Appendix 2 for locality details).

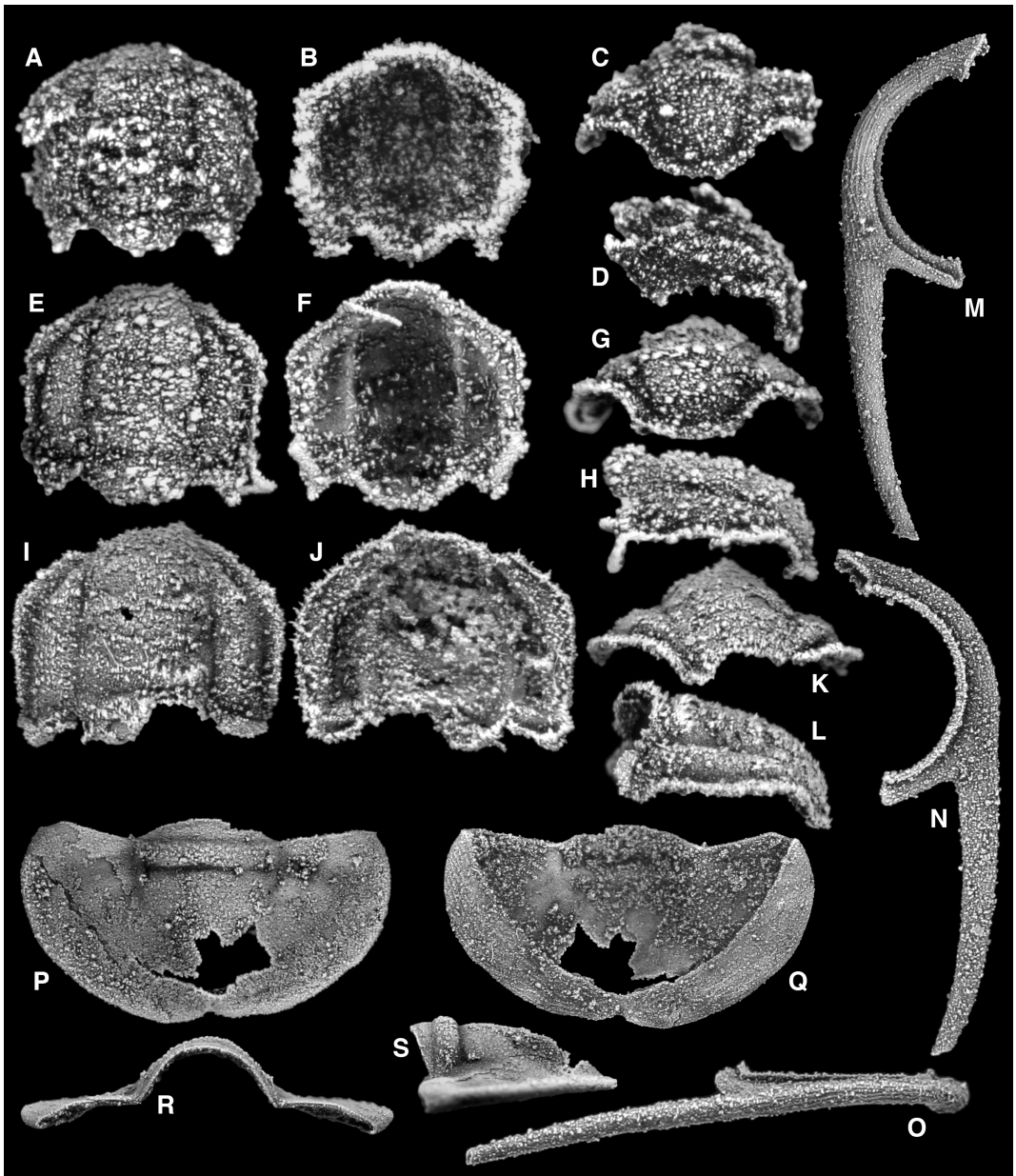


Fig. 4. Silicified sclerites of *Bathynotus* sp. indet. **A-D**, coarsely silicified cranium in dorsal, ventral, anterior, and right lateral views, FMNH PE58136, from ICS-1173, x25. **E-H**, coarsely silicified cranium in dorsal, ventral, anterior, and right lateral views, FMNH PE58137, from ICS-1173, x20. **I-L**, coarsely silicified cranium in dorsal, ventral, anterior, and right lateral views, FMNH PE58138, from ICS-10252, x15. **M-O**, right librigena in ventral, dorsal, and right lateral views, FMNH PE58135, from ICS-1173, x10. **P-S**, pygidium in dorsal, ventral, anterior, and left lateral views, FMNH PE58134, from ICS-1290, x10. All from the Combined Metals Member, Pioche Formation, Lincoln County, Nevada (see Appendix 2 for locality details).

specimens (generously sent by Professors Jin Peng [Nanjing University] and Yuanlong Zhao [Guizhou University]) plus a specimen formerly housed in the ICS collections (Fig. 1D) further bolstered the South China sample size for the

morphometric analysis (Appendix 1).

Australia

One complete and several fragmentary specimens of *Bathynotus* have been recovered from the

Abbreviation	Variable
GL	Glabella length (sag.)
BGW	Basal glabella width (tr.)
GWSO	Glabella width at contact between SO and axial furrow (tr.)
GWS1	Glabella width at contact between S1 and axial furrow (tr.)
GWS2	Glabella width at contact between S2 and axial furrow (tr.)
LOL	Length of LO at axial furrow (exsag.)
L1L	Length of L1 at axial furrow (exsag.)
L2L	Length of L2 at axial furrow (exsag.)
FAL	Frontal area length (sag.)
PWW	Posterior wing width (tr.)
GSL	Genal spine length

Table 1. Length measurements and their abbreviations used in morphometric analysis.

lower Arthur Creek Formation at two localities approximately 40 km southeast of Elkedra, Northern Territory, Australia (Öpik 1956, 1975; Shergold & Whittington 2000). The specimens occur in pebbles of siltstone float and their exact stratigraphic provenance cannot be determined, but an Ordian or Early Templetonian age is likely. Öpik (1956, pp. 43-44) identified the specimens as “*Bathynotus* cf. *holopyga*” [sic], and noted that they differed from Laurentian *B. holopygus* by “its simpler pygidium and, perhaps, ornament”. He considered the Australian material to represent a new species (see also Öpik 1975, p. 12, referred to as “*Bathynotus* sp. nov.”). However, Shergold & Whittington (2000) and subsequent workers assigned the material to *B. holopygus* without question. Two of the specimens figured by Shergold & Whittington (2000) were appropriate for inclusion in the morphometric analysis (Appendix 1).

Siberia: Siberian Platform

Bathynotus namanensis Lermontova, 1940 is known from the Toyonian (*Namanoia* Zone) at several sites on the southern Siberian Platform (Lermontova 1940; Ogienko *et al.* 1974; Astashkin *et al.* 1991; Ogienko & Garina 2001). Lermontova (1940) stated that *B. namanensis* differed from *B. holopygus* in having a slightly narrower anterior glabella, weaker glabella furrows (but with a visible S2), and a smooth surface, but the species were placed into synonymy by Yuan *et al.* (2002). Data from six specimens figured in the literature as *B. namanensis* (including the lectotype; Fig. 3H) were included in the morphometric analysis (Appendix 1).

Bathynotus anabarensis Lazarenko, 1958 is known from the late Amgan (*Tomagnostus fissus-Paradoxides sacheri* Zone) Shumnoy Formation on the Sukharikha River in the Anabar-Sinsk Facies of the northwestern Siberian Platform (Lazarenko 1958; Astashkin *et al.* 1991, p. 86) and from Novaya Zemlya (Lermontova 1940; Lazarenko 1958). Only the cranidium is known. Seven of the cranidia figured by Lazarenko (1958) were included in the morphometric analysis

(Appendix 1).

Ogienko (in Ogienko & Garina 2001) named *B. angularis* based on cranidia from the Amgan (*Chondranomocare-Kounamkites* Zone) Udachny Formation in the Daldyn River basin (a tributary of the Markha River), in the Anabar-Sinsk Facies of the central Siberian Platform. Data from the three figured cranidia (including the holotype) were included in the morphometric analysis (Appendix 1).

Siberia: Altay-Sayan Foldbelt

Bathynotus granulatus Lermontova, 1940, from the “Middle” Cambrian (Amgan?) of the Minusinsk region (Lermontova 1940; Lazarenko 1958) was also considered synonymous with *B. holopygus* by Yuan *et al.* (2002). Data from the two cranidia figured in the literature as *B. granulatus* (including the lectotype) were included in the morphometric analysis (Appendix 1).

Bathynotus fortis Semashko, 1969 from the Amgan Mundybash Formation in the Kuznetsk Alatau (Astashkin *et al.* 1995) is known from small cranidia only. Data from one of the two figured specimens (the holotype) were included in the morphometric analysis (Appendix 1).

Bathynotus rotundus Semashko, 1969 is also known from the Mundybash Formation in the Kuznetsk Alatau (Astashkin *et al.* 1995), and is represented by tiny cranidia only. Data from both figured specimens (including the holotype) were included in the morphometric analysis (Appendix 1).

MORPHOMETRIC ANALYSIS

Material

Traditional morphometric length measurements (Table 1) and qualitative data were extracted from images of 96 well preserved *Bathynotus* specimens, representing all nine putative species and including material from eastern Laurentia (Vermont), western Laurentia (Nevada), South China, Australia (Northern Territory), and Siberia (above; Appendix 1). The sample includes specimens preserved in fine-grained siliciclastics (Vermont, Nevada, South China, and Australia)

	PC1	PC2	PC3	PC4	PC5	PC6	PC7	PC8
Eigenvalue	60.310	0.319	0.103	0.048	0.035	0.022	0.011	0.006
% Variance Explained	99.11	0.52	0.17	0.08	0.06	0.04	0.02	0.01
Component Loadings								
GL	3.910	-0.441	0.054	0.000	0.021	-0.039	-0.010	0.011
BGW	3.903	0.114	-0.214	0.030	-0.016	-0.044	0.036	-0.012
GWSO	3.475	0.129	-0.039	-0.046	-0.049	0.061	-0.042	0.044
GWS1	2.929	0.146	0.088	0.029	0.006	-0.001	-0.053	-0.054
GWS2	2.710	0.223	0.190	-0.022	0.045	-0.015	0.052	0.017
LOL	0.774	-0.050	-0.076	0.009	0.146	0.082	0.007	-0.007
L1L	0.893	-0.133	0.019	-0.113	-0.072	0.064	0.040	-0.034
L2L	0.620	-0.065	0.051	0.176	-0.060	0.059	0.023	0.003

Table 2. Principal Component Analysis of the eight glabellar dimensions.

and in carbonates (crackout material from Siberia and silicified sclerites from Nevada). Many specimens from Vermont and South China have been tectonically distorted to various degrees. Morphometric data were not extracted from images of specimens that have suffered gross tectonic distortion. However, data from specimens that have suffered minor tectonic distortion (but are otherwise well preserved) were included in the analysis in order to test the claim that some purported species of *Bathynotus* may represent tectonically deformed members of other species (see Shergold & Whittington 2000, p. 7). Specimens preserved in siliciclastics have suffered compactional deformation, which is known to inflate the observed morphological variation of trilobite species (e.g., Webster & Hughes 1999). However, given that all morphologically mature *Bathynotus* specimens from outside Siberia are preserved in this condition, the inclusion of compacted material in the analysis is necessary.

Specimens mentioned in this paper are housed in the collections of the American Museum of Natural History (AMNH), the Commonwealth Palaeontological Collection (CPC, Geoscience Australia, Canberra), the Field Museum of Natural History, Chicago (FMNH), the Institute for Cambrian Studies (ICS, Department of the Geophysical Sciences, University of Chicago), the Nanjing Institute of Geology and Palaeontology (NIGP, Chinese Academy of Science), the Smithsonian Institution, Washington D.C. (USNM), and Yale Peabody Museum (YPM, Yale University). Stratigraphic information for individual collections from Nevada is recorded in the ICS database, available from the author upon request. Information regarding data sources for all specimens is provided in the appendices.

Methods

Morphological similarity between specimens was assessed through a series of multivariate

and bivariate morphometric analyses of the quantitative variables. These analyses investigated 1.) whether specimens formed distinct clusters in morphospace, each cluster representing a putative species; and 2.) whether those clusters were diagnosable in terms of statistically discrete character states recognised within the continuous morphometric variables.

Multivariate analyses involved a principal component analysis (PCA) of length measurements (Table 1). Separate analyses were conducted on variables describing glabellar shape and cranial shape (the former being a subset of the latter). Many cranidia are incompletely preserved. Specimens for which at least one variable is unknown cannot be included in a PCA which involves that variable. To maximise sample size, incomplete length measurement(s) on some otherwise usable specimens were therefore estimated (e.g., obtaining the full transverse width of the glabella across SO by doubling the distance from the distal tip of SO to the sagittal axis). Such estimated values were only included in the analysis if they were replicable with a high degree of consistency; the value was otherwise treated as unknown and the specimen excluded from the PCA. Genal spine length was known for too few specimens to warrant its inclusion in a multivariate analysis. Results are presented here for PCA utilising the variance-covariance matrix among untransformed variables (because this involves least data modification): similar results and conclusions were attained based on analyses utilising the correlation matrix and/or log-transformed variables (not shown).

Bivariate analyses involved plotting the natural logarithm of each variable against the natural logarithm of sagittal glabellar length. Specimens were assigned to groups based on their clustering in the multivariate analysis. The number of clusters served as an hypothesis of the number of putative character states exhibited in

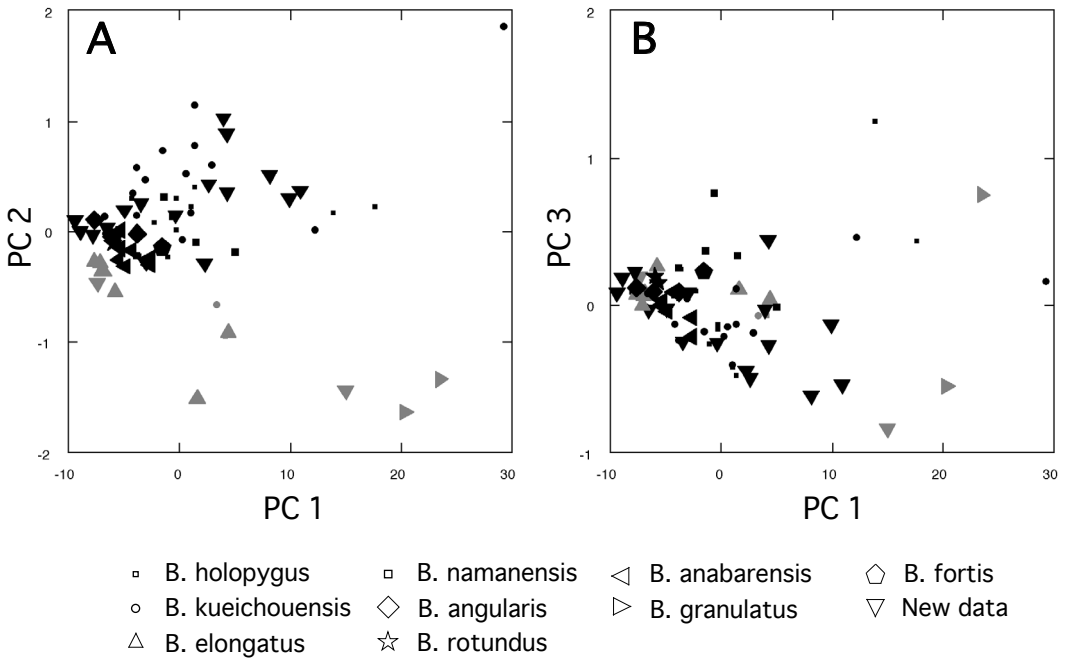


Fig. 5. Morphospace defined by the first three principal components of the PCA of eight glabellar dimensions (Table 1). **A.** PC1 versus PC2. **B.** PC 1 versus PC3. Symbols indicate previous species assignment; shading indicates clustering identified herein (grey = “*granulatus*” cluster; black = “*holopygus*” cluster). See Table 2 and text for details and interpretation.

that variable. For variables that were not included in the multivariate analysis (e.g., genal spine length) the number of distinct regression lines that appeared to be represented in the data distribution served as an hypothesis of the number of putative character states exhibited in that variable. Reduced major axis (RMA) regression lines were fitted to each putative character state, and the statistical significance of among-state difference in slope and intercept of the RMA regression line was assessed through bootstrap resampling of the data (2000 replicates). Regression lines that were significantly different in slope and/or intercept at 95% confidence were considered to represent discrete states within the variable. RMA regression and the bootstrapping procedure was conducted using the PAST software package (Hammer *et al.* 2001; freely available at <http://folk.uio.no/ohammer/past/>).

Results: Multivariate analyses

Glabellar dimensions. In a PCA of the eight glabellar dimensions, the first principal component (PC1; Table 2) accounts for 99% of the variance in the data and is associated with high, positive loadings for glabellar length and all glabellar width variables (less so for width across S1 and S2 than across SO and the base of the glabella). The contribution of the variables for length of

LO, L1, and L2 are positive but of much lower magnitude. Each loading on PC1 reflects the mean value and the variance of the original variable, and PC1 relates primarily to size. The second principal component (PC2; Table 2) accounts for 0.5% of the variance in the data, and is associated with a strong negative loading for glabellar length (with weak negative loadings for the lengths of LO, L1, and L2) contrasted with strong positive loadings for measures of glabellar width (increasingly strong contributions for more anterior width measures).

Specimens form two clusters in a morphospace defined by PC1 and PC2 (Fig. 5A). The two specimens of *B. granulatus* from Siberia, specimens figured as *B. elongatus* from South China, the articulated *Bathynotus* specimen from Nevada (Fig. 1C), plus one South China cranidium figured as *B. holopygus* (gkdo03; almost coincident with the scores of the *B. elongatus* holotype) and (arguably) one South China cranidium figured as *B. kueichouensis* (T010) all exhibit much lower scores on PC2 relative to score on PC1 compared to all other specimens. They are therefore characterised by possession of a proportionally narrower glabella (especially across S1 and S2). For ease of reference, this suite of specimens is henceforth referred to as the “*granulatus*” cluster. The remaining specimens have higher

	PC1	PC2	PC3	PC4	PC5	PC6	PC7	PC8	PC9	PC10
Eigenvalue	79.114	0.514	0.197	0.105	0.070	0.050	0.018	0.009	0.007	0.005
% Variance Explained	98.78	0.64	0.25	0.13	0.09	0.06	0.02	0.01	0.01	0.01
Component Loadings										
GL	4.394	0.487	-0.187	0.005	0.022	-0.028	-0.021	0.009	-0.021	0.000
BGW	4.375	-0.111	0.172	0.181	-0.032	0.004	-0.055	0.004	0.014	0.017
GWSO	3.899	-0.180	0.037	0.024	-0.076	0.031	0.071	0.021	-0.032	-0.028
GWS1	3.316	-0.196	-0.045	-0.074	0.076	0.047	0.007	-0.068	-0.014	0.015
GWS2	3.133	-0.305	-0.121	-0.155	0.023	-0.050	-0.022	0.038	0.032	0.002
LOL	0.825	0.020	0.080	0.062	0.089	-0.167	0.041	-0.021	0.016	-0.018
L1L	0.982	0.136	-0.068	-0.022	-0.180	-0.012	0.038	-0.030	0.043	0.010
L2L	0.741	0.097	-0.060	0.085	0.122	0.114	0.047	0.014	0.043	-0.005
FAL	0.347	0.027	0.006	-0.022	-0.022	0.038	-0.059	-0.025	0.016	-0.057
PWW	1.565	0.267	0.316	-0.172	0.021	0.025	0.009	0.008	0.007	0.004

Table 3. Principal Component Analysis of the ten cranial dimensions.

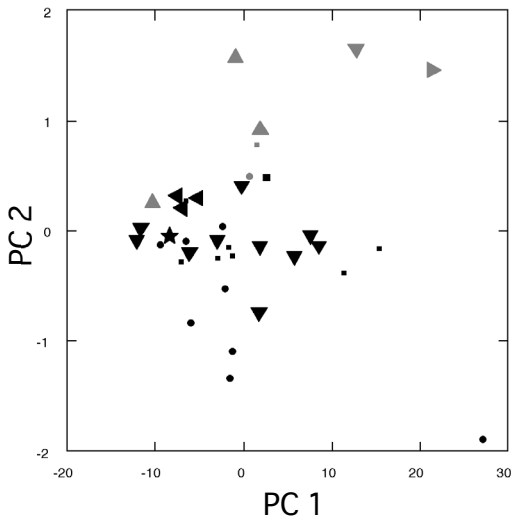


Fig. 6. Morphospace defined by the first two principal components of the PCA of ten glabellar dimensions (Table 1). Symbols indicate previous species assignment (key given in Fig. 5); shading indicates clustering identified herein (grey = “granulatus” cluster; black = “holopygus” cluster). See Table 3 and text for details and interpretation.

scores on PC2 (proportionally wider glabella, especially across S1 and S2) and form a cloud with generally increasing variation along PC2 relative to score along PC1. This group includes all specimens of *B. holopygus* (except gkdo03), *B. kueichouensis* (except T010), *B. fortis*, *B. anabarensis*, *B. namanensis*, *B. angularis* and *B. rotundus*, plus specimens from Nevada, and is henceforth referred to as the “*holopygus*” cluster. Specimens of *B. anabarensis* lie along the edge of this group on the low-PC2 score end. Each cluster consists of all specimens of a group of previously named species (with only two specimens previously misassigned, above). Despite explaining only a small proportion of the total variance, PC2 is therefore interpreted to have

biological significance.

Higher PCs each explain <0.2% of the variance in the data (Table 2); all show cones of increasing variation relative to score on PC1, and no distinct separation among putative morphotypes is present (e.g., Fig. 5B). These PCs are not further interpreted here.

Discriminant function analysis of the eight glabellar dimensions reveals that the two groups recognised within the PCA (the “*granulatus*” and “*holopygus*” clusters) are significantly different from each other (eigenvalue = 1.062; Wilk’s Lambda = 0.485; 8 degrees of freedom; $p < 0.0005$).

A PCA of glabellar dimensions excluding glabellar width across S2 and length of L2 was also conducted, because S2 is not clearly incised (and L2 length is consequently not determinable) on many specimens. This increased sample size in the analysis, but the results were consistent with those presented above and are therefore not shown here.

Cranial dimensions. Results of the multivariate PCA of the ten cranial dimensions are consistent with those of the PCA of the eight glabellar dimensions (above), although sample size is smaller. PC1 again accounts for 99% of the variation in the data, and is associated with high, positive loadings for glabellar length and all glabellar width variables (less so for width across S1 and S2 than across SO and the base of the glabella; Table 3). The contribution of the variables for length of LO, L1 and L2, and for frontal area length and posterior wing width are positive but of much lower magnitude. PC1 again relates primarily to size.

PC2 accounts for 0.6% of the variance in the data, and is associated with a strong positive loading for glabellar length (with weak positive loadings for the lengths of the frontal area, LO, L1 and L2, and for the width of the posterior

Characters	State	Group	n	RMA r	RMA Slope	RMA Intercept
lnBGW vs. lnGL	Proportionally narrow BGW	"granulatus" cluster	16	0.998	1.199	-0.677
	Proportionally wide BGW	"holopygus" cluster	77	0.987	1.189	-0.435
lnGWSO vs. lnGL	Proportionally narrow GWSO	"granulatus" cluster	15	0.999	1.167	-0.719
	Proportionally wide GWSO	"holopygus" cluster	75	0.991	1.163	-0.498
lnGWS1 vs. lnGL	Proportionally narrow GWS1	"granulatus" cluster	15	0.998	1.135	-0.822
	Proportionally wide GWS1	"holopygus" cluster	73	0.991	1.127	-0.570
lnGWS2 vs. lnGL	Proportionally narrow GWS2	"granulatus" cluster	13	0.999	1.126	-0.884
	Proportionally wide GWS2	"holopygus" cluster	61	0.990	1.149	-0.690
lnGSL vs. lnGL	Proportionally short GSL	lower cluster	12	0.953	1.312	-0.638
	Proportionally long GSL	upper cluster	11	0.979	1.148	0.549

Table 4. Comparison of slopes and intercepts of reduced major axis (RMA) regression lines of putative states of continuous variables versus sagittal glabellar length (see Figs 7, 8). For all characters, putative states significantly differed in RMA intercept at 95% confidence (based on 2000 bootstrap replicates). All RMA slopes except proportionally long GSL are significantly > 1.0 at 95% confidence (based on 2000 bootstrap replicates). Abbreviations for variables are given in Table 1. Other abbreviations: n, sample size within group; r, correlation coefficient. See text for details and interpretation.

wing) contrasted with strong negative loadings for measures of glabellar width (increasingly strong contributions for more anterior width measures; Table 3). Other than the switch in sign (which is arbitrary in the ordination) PC2 in this analysis is equivalent to PC2 in the analysis of glabellar dimensions (above); the distributions of specimens and putative species are also consistent across the two analyses (Fig. 6).

Higher PCs each explain <0.25% of the variance in the data (Table 3); all show cones of increasing variation relative to score on PC1, and no distinct separation among putative morphotypes is present (data not shown).

Results: Bivariate analyses and discrete (qualitative and meristic) data

Statistical analyses of bivariate plots plus consideration of discrete (qualitative and meristic) data confirm the distinction between the "granulatus" and "holopygus" clusters recognised in the exploratory multivariate analyses (above), and reveal that the "holopygus" cluster can be further subdivided into three taxa based on variables not included in the multivariate analyses.

Basal glabellar width versus glabellar length. A RMA regression line through the data for specimens assigned to the "granulatus" cluster exhibits an intercept that is significantly different from that of a RMA regression line through the data for specimens assigned to the "holopygus" cluster (Table 4). However, several specimens assigned to the "holopygus" cluster based on the results of the multivariate analysis fall close to or on the regression line for the "granulatus" cluster (e.g., the two smallest specimens and

several large specimens; Fig. 7A); assignment of these few specimens to either regression line is arbitrary. Basal glabellar width (proportional to glabellar length) is therefore typically but not universally useful for discriminating the two groups of specimens recognised in the multivariate analysis.

Glabellar width across SO versus glabellar length. A RMA regression line through the data for specimens assigned to the "granulatus" cluster exhibits an intercept that is significantly different from that of a RMA regression line through the data for specimens assigned to the "holopygus" cluster (Table 4). Visual distinction between the two regression lines (Fig. 7B) is clearer than in the plot of basal glabellar width versus glabellar length (above), although the two smallest specimens assigned to the "holopygus" cluster based on the results of the multivariate analysis again fall close to or on the regression line for the "granulatus" cluster. Except at the smallest sampled cranial size, glabellar width across SO (proportional to glabellar length) is therefore useful for discriminating the two groups of specimens recognised in the multivariate analysis.

Glabellar width across S1 versus glabellar length. A RMA regression line through the data for specimens assigned to the "granulatus" cluster exhibits an intercept that is significantly different from that of a RMA regression line through the data for specimens assigned to the "holopygus" cluster (Table 4). Visual distinction between the two regression lines is clear (Fig. 7C), although some specimens of *B. anabarensis* (assigned to the "holopygus" cluster based on the results of the

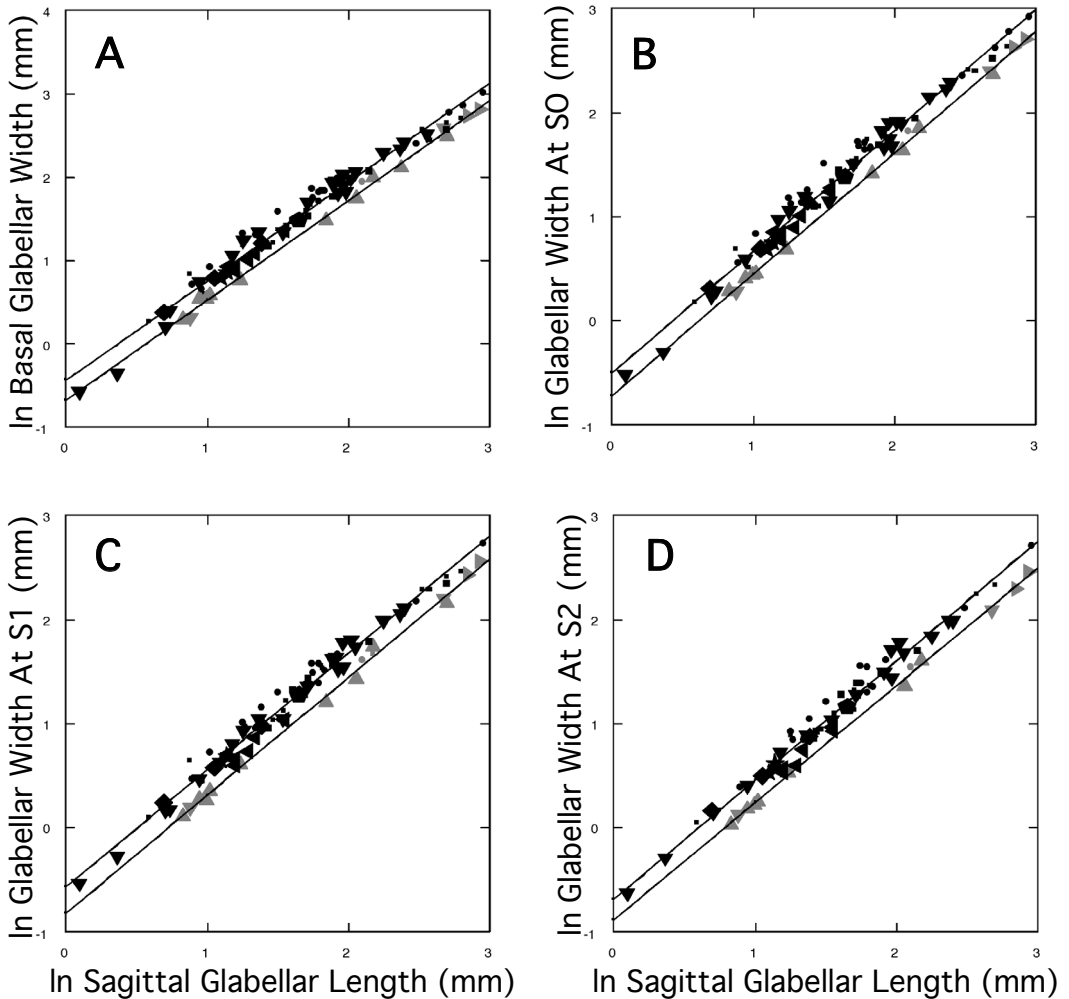


Fig. 7. Bivariate plots of continuous morphometric variables versus sagittal glabellar length, with reduced major axis regression lines shown for each putative state. **A**, Basal glabellar width versus sagittal glabellar length. **B**, Glabellar width at SO versus sagittal glabellar length. **C**, Glabellar width at S1 versus sagittal glabellar length. **D**, Glabellar width at S2 versus sagittal glabellar length. Symbols indicate previous species assignment (key given in Fig. 5); shading indicates putative states identified herein (grey = proportionally narrow [*“granulatus”* cluster], lower regression line; black = proportionally wide [*“holopygus”* cluster], upper regression line). See Table 4 and text for details and interpretation.

multivariate analysis) fall close to the regression line for the *“granulatus”* cluster. The smallest cranidia fall along the regression line of the *“holopygus”* cluster.

Glabellar width across S2 versus glabellar length. A RMA regression line through the data for specimens assigned to the *“granulatus”* cluster exhibits an intercept that is significantly different from that of a RMA regression line through the data for specimens assigned to the *“holopygus”* cluster (Table 4). Visual distinction between the two regression lines is clear (Fig. 7D) although again some specimens of *B. anabarensis*

(assigned to the *“holopygus”* cluster based on the results of the multivariate analysis) fall close to the regression line for the *“granulatus”* cluster. The smallest cranidia fall along the regression line of the *“holopygus”* cluster.

Length of glabellar lobes versus glabellar length. There is no differentiation between the *“granulatus”* and *“holopygus”* clusters in the exsagittal lengths of LO, L1 or L2 when plotted against sagittal glabellar length; nor can any named *Bathynotus* species be consistently distinguished by these variables (data not shown).

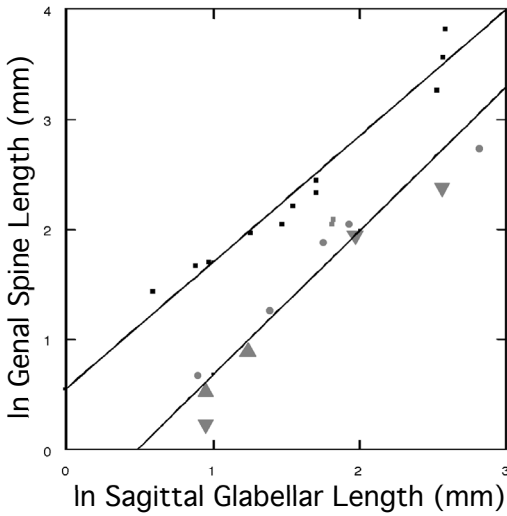


Fig. 8. Bivariate plot of genal spine length versus sagittal glabellar length, with reduced major axis regression lines shown for each putative state. Symbols indicate previous species assignment (key given in Fig. 5); shading indicates putative states identified herein (grey = proportionally short genal spine, lower regression line; black = proportionally long genal spine, upper regression line). See Table 4 and text for details and interpretation.

Non-glabellar cranial features. There is no consistent differentiation among named species or between the “*granulatus*” and “*holopygus*” clusters in sagittal length of the frontal area, in width of the posterior wing, or in orientation of the posterior wing of the fixed cheek relative to sagittal glabellar length (data not shown).

Genal spine length. Data fall along two distinct regression lines in a plot of genal spine length versus sagittal glabellar length (Fig. 8). The lower regression line, characterising the specimens with proportionally short genal spines, includes specimens that have been figured as *B. elongatus* (e.g., Peng *et al.* 2009, fig. 1g) and *B. kueichouensis* (e.g., Yuan *et al.* 2002, pl. 8, figs 1, 4), in addition to the two specimens from Australia (Shergold & Whittington 2000, figs 2a, b). The upper regression line, characterising the specimens with proportionally longer genal spines, includes specimens that have been figured as *B. holopygus* from Vermont (e.g., Fig. 1B) and South China (e.g., Yuan *et al.* 2002, pl. 7, figs 1, 2, 5). The RMA regression lines are significantly different (Table 4), and genal spine length is considered to be a character pertinent to species diagnosis.

Granular ornament. A granular ornament is absent from *Bathynotus* cranidia smaller

than 2.5 mm long (sag.), but is developed on virtually all cranidia longer than 8 mm (sag.). Expression of this ornament is variable among large cranidia (e.g., ranging from clear, relatively coarse granules [Fig. 1B] to much a more subtle, fine ornament [Whittington 1988, pl. 52, fig. 4] on similar-sized specimens of *B. holopygus* from the same locality). This variation is at least partially influenced by preservation: in some cases a fine granulation is evident on the external surface of sclerites but not on the internal surface (e.g., compare the testate trunk to the exfoliated cranidium in Fig. 1D). Allowing for such taphonomic (and biological) variation, size-related development of the granular ornament appears to be a general feature of *Bathynotus* ontogeny. The only exception appears to be the consistent absence of granular ornament from cranidia of *B. namanensis* even at large size (e.g., Fig. 3H): this species can therefore be uniquely diagnosed based on this condition.

Number of axial rings defined on the pygidial axis. Well preserved pygidia are known from relatively few *Bathynotus* specimens. Virtually all exhibit one axial ring plus an undifferentiated terminal piece. Rarely, a second axial ring is also expressed (Whittington 1988, pl. 52, fig. 1; Yuan *et al.* 2002, pl. 9, fig. 6). Given that these specimens belong to different putative species (bearing long and short genal spines, respectively) the presence of two axial rings in the pygidium does not constitute a character which can be used to consistently diagnose a species that would include more than one specimen.

Pygidial notch. The posterior margin of the pygidium of some *Bathynotus* specimens forms a broad, continuous, posteriorly-projecting curve. On other specimens the posterior pygidial margin bears a subtle “notch” where it is deflected slightly anteriorly as it crosses the sagittal axis (the form of the posterior margin then resembles a broad, rounded “W”; Fig. 1D). It is unlikely that the presence of the notch is a taphonomic artifact associated with compactional deformation, because it is present on a non-compacted silicified pygidium (Fig. 4P-S).

A pygidial notch is present on small specimens (sagittal glabellar length < 5 mm) figured as *B. holopygus* (from South China; e.g., Yuan *et al.* 2002, pl. 7, figs 2, 5 [specimen on right]), is weak or absent on specimens between 5 mm and 6 mm in sagittal glabellar length (also from South China; e.g., Yuan *et al.* 2002, pl. 7, fig. 1; Peng *et al.* 2009, fig. 1b), and is consistently absent on larger specimens (from Vermont; e.g., Fig. 1A, B). (Large specimens from South China

and small specimens from Vermont are unknown but, given that the transition from presence to absence of the notch is seen in South China material, plus the morphometric support for conspecificity of the South China and Vermont *B. holopygus* specimens [above], the Vermont material is deemed to represent an extension of the ontogenetic trends detected in the South China material.) Similarly, a pygidial notch is apparently present on small specimens of *B. elongatus* from South China (Y. Zhao, personal communication January 2009; although the condition is unclear in the figured material) but appears to be absent on larger specimens figured as *B. elongatus* (e.g., Yuan *et al.* 2002, pl. 9, figs 1, 3; although the pygidial margin is sometimes sagittally disrupted by a fracture).

Specimens assigned to *B. kueichouensis* consistently have a pygidial notch, even at large sizes (sagittal glabellar length > 6 mm; e.g., Yuan *et al.* 2002, pl. 8, figs 1, 3, 4, pl. 9, fig. 5). Although the posterior pygidial margins on the Australian specimens are slightly worn, a subtle sagittal notch might be present (see the sagittally converging terrace lines in the pygidial doublure of CPC 34706; Shergold & Whittington 2000, fig. 2d).

Summary

Results of the various morphometric analyses (above) together support the presence of four species of *Bathynotus* in this sample of 96 specimens: *B. granulatus*, *B. holopygus*, *B. kueichouensis* and *B. namanensis*. Each species is diagnosed by a unique combination of character states that unites all semaphoronts within that species to the exclusion of all semaphoronts belonging to other species, and therefore fulfills the criteria of the phylogenetic species concept (above).

Bathynotus granulatus is diagnosed by having a significantly proportionally narrower glabella (particularly across S1 and S2) than all other species. It bears proportionally short genal spines throughout ontogeny (as does *B. kueichouensis*), loses a pygidial notch through ontogeny (as does *B. holopygus*), and develops a granular ornament (as do *B. holopygus* and *B. kueichouensis*). *Bathynotus elongatus* from South China is a junior synonym of *B. granulatus*.

Bathynotus kueichouensis is diagnosed by having a significantly proportionally wider glabella (particularly across S1 and S2) than *B. granulatus*, having proportionally short genal spines throughout ontogeny (as does *B. granulatus*), and retaining a pygidial notch through ontogeny. It develops a granular ornament (as do *B. holopygus* and *B. granulatus*).

Bathynotus holopygus is diagnosed by having a significantly proportionally wider glabella (particularly across S1 and S2) than *B. granulatus*, and having proportionally long genal spines throughout ontogeny. It loses a pygidial notch through ontogeny (as does *B. granulatus*), and develops a granular ornament (as do *B. granulatus* and *B. kueichouensis*).

Finally, *B. namanensis* is diagnosed by lacking a granular ornament at large cranial size (sagittal cephalic length > 9 mm). It is indistinguishable from *B. holopygus* and *B. kueichouensis* in glabellar and cranial dimensions.

Tectonic deformation of specimens has been claimed to account for some species-level distinctions within the genus (Shergold & Whittington 2000, p. 7). However, such deformation cannot account for the interspecific differences documented above in presence or absence of granular ornament or pygidial notch, or in proportional length of the genal spines.

A description and the revised stratigraphic and geographic distribution of each of these species are presented below. It is clear from the above analyses and summary that some of the species are diagnosed by a unique combination of (non-unique) character states. This means that many isolated sclerites cannot be identified to species level. For example, *B. holopygus* and *B. kueichouensis* cannot be distinguished from one another based on cranial morphology alone, and a librigena bearing a proportionally short genal spine cannot be unequivocally assigned to *B. granulatus* or to *B. kueichouensis* unless it remains associated with the cranidium.

Many of the Siberian species recognised by previous workers appear to have been diagnosed on shape differences that are primarily attributable to size differences (i.e., resulting from ontogenetic allometry; see below). Some differences in glabellar proportions are evident in pairwise comparisons between similarly sized specimens of the various "species" described from Siberia, but these differences are bridged by specimens of intermediate morphology and cannot serve to uniquely diagnose the named taxa.

SYSTEMATIC PALAEOONTOLOGY

Family BATHYNOTIDAE Hupé, 1953

Bathynotus Hall, 1860

1860 *Bathynotus*; Hall, p. 117-118.

1860 *Pagura*; Emmons, p. 280.

1861 *Bathynotus*; Hall, p. 371.

1886 *Bathynotus*; Walcott, p. 191.

1889 *Bathynotus*; Miller, p. 532.

- 1910 *Bathynotus*; Grabau & Shimer, p. 262.
 1935 *Bathynotus*; Kobayashi, p. 140.
 1938 *Bathynotus*; Resser & Howell, p. 229.
 1940 *Bathynotus*; Lermontova, p. 134.
 1951 *Bathynotus*; Lermontova, p. 96-97.
 1954 *Bathynotus*; Kobayashi, p. 31-32, 39.
 1958 *Bathynotus*; Lazarenko, p. 15-16.
 1959 *Bathynotus*; Lochman-Balk in Harrington *et al.*, p. O216.
 1960 *Bathynotus*; Balashova & Suvorova in Chernysheva (ed.), p. 128.
 1963 *Bathynotus*; Lu *et al.*, p. 61.
 1965 *Bathynotus*; Lu *et al.*, p. 93.
 1978 *Bathynotus*; Yin & Lee, p. 432.
 1981 *Bathynotus*; Zhang, p. 154.
 1984 *Bathynotus*; Sun, p. 349.
 1990 *Bathynotus*; Zhao *et al.*, p. 46.
 2000 *Bathynotus*; Shergold & Whittington, p. 1-4.
 2002 *Bathynotus*; Yuan *et al.*, p. 84-86.
 2003 *Bathynotus*; Jell in Jell & Adrain, p. 347, 468.

Type species. Peltura (Olenus) holopyga Hall, 1859a (designated by Hall 1860).

Other species. Bathynotus granulatus Lermontova, 1940; *Bathynotus kueichouensis* Lu in Wang, 1964; and *Bathynotus namanensis* Lermontova, 1940.

Discussion. With its proportionally wide axis, macropleuraleleventh thoracic segment, fused T11-T13 unit (Fig. 1), and very unusual arrangement of ventral sutures (below), *Bathynotus* is a distinctive trilobite genus of controversial affinities. It has been variously assigned to the ptychoparioid Family Komaspidae (now the Elviniidae; Kobayashi 1935, 1954), the redlichine Family Chengkouaspidae (Jell in Jell & Adrain 2003), and the Family Bathynotidae (Hupé 1953). The Bathynotidae has in turn been considered to represent a redlichoid family (Hupé 1953; Shergold & Whittington 2000; Yuan *et al.* 2002), a monofamilial redlichoid suborder Bathynotina (Lochman-Balk in Harrington *et al.* 1959), or to be of uncertain ordinal affinity (Fortey in Whittington *et al.* 1997). Jell (in Jell & Adrain 2003) provided no justification for assignment to the Chengkouaspidae and, pending a broad study of the phylogenetic placement of the genus (which is beyond the scope of the present paper), provisional assignment of *Bathynotus* to the Bathynotidae is followed here.

The bizarre condition of the cephalic sutures in *B. holopygus*, in which the anterior branches of the dorsal facial sutures and the ventral sutures converge to form a broad "X"-shape

at the anterior sagittal cephalic margin, was thoroughly described by Whittington (1988, pp. 581-584, 601; also Rasetti 1952, pp. 890-891, pl. 1, fig. 5; Harrington *et al.* 1959, pp. O64-O65, O67; Whittington in Whittington *et al.* 1997, pp. 38-39). Similar morphology occurs in *B. kueichouensis* (e.g., Yuan *et al.* 2002, pl. 8, fig. 2). Such an arrangement is extremely unusual among trilobites (some specimens of *Shergoldia laevigata* Zhu *et al.* 2007 show an analogous arrangement), and contributes to the difficulty of higher-level systematic placement of the genus. The homology of the anteriorly-converging ventral sutures is uncertain: either the hypostome is subrectangular and fused to an anteriorly-tapering, triangular rostral plate (in which case the ventral sutures are the connective sutures and the hypostomal suture is lost), or the hypostome has an anteriorly tapering, triangular anterior projection and the rostral plate is absent (in which case the ventral sutures are the hypostomal suture). Irrespective of sutural homology, the hypostome would have been conterminant and firmly braced (Whittington 1988, p. 602). Such a condition, along with the relatively wide (tr.) axial region of the body, has been used to argue that *Bathynotus* may have been a pelagic predator (Shergold & Whittington 2000, p. 8). Given the relatively large size of mature individuals (Fig. 1), a nektonic rather than pelagic life mode is perhaps more likely. Whether swimming above the seafloor at maturity (hunting or otherwise) was facultative or obligatory is unknown.

Peng *et al.* (2009, p. 100) considered *Bathynotellus yermolaevi* Lermontova, 1940 from Novaya Zemlya, Siberia (type species of *Bathynotellus* Lermontova, 1940), to be synonymous with *Bathynotus holopygus*. The other species in the genus, *Bathynotellus jershovi* Solovov in Solovov & Grikurov, 1979, was not mentioned by Peng *et al.* (2009), and the status of the genus *Bathynotellus* was left ambiguous. However, *Bathynotellus yermolaevi* differs markedly from *B. holopygus* (and from all species of *Bathynotus*) in having 1.) a frontal area that is as wide or wider (tr.) than the basal glabella width; 2.) a short (exsag.) strip of exoskeleton between the proximal portion of the palpebral lobes and the anterior cranial border (i.e., γ is more abaxially located along the palpebral ridge); 3.) a long posterodorsally oriented occipital spine (approximately as long as the cranium); 4.) short (sentate) pleural spines on thoracic segments anterior to T11; and 5.) an elongate (sag.), subtriangular pygidium with an axis bearing at least three, if not four, axial rings plus a terminal piece. These pronounced differences demonstrate that synonymy with

Bathynotus holopygus is unsupported, and both *Bathynotellus* and *Bathynotellus yermolaevi* are here re-established as valid taxa.

Bathynotus holopygus (Hall, 1859a) (Fig. 1A-B)

- 1859a *Peltura (Olenus) holopyga*; Hall, p. 61-62, fig. 3.
 1859b *Peltura (Olenus) holopyga*; Hall, p. 528-529, text-fig.
 1860 *Paradoxides? quadrispinosus*; Emmons, p. 80, text-fig. 57.
 1860 *Paradoxides (Pagura) quadrispinosus*; Emmons, p. 280.
 1860 *Bathynotus holopyga*; Hall, p. 118-119, text-fig.
 1861 *Peltura (Olenus) holopyga*; Barrande, p. 278-280, pl. 5, figs 9, 10.
 1861 *Bathynotus holopyga*; Hall, p. 371-372, pl. 13, fig. 3.
 1886 *Bathynotus holopyga*; Walcott, p. 191-193, pl. 31, figs 1, 1a.
 1889 *Bathynotus holopyga*; Miller, p. 532, text-fig. 970.
 1890 *Bathynotus holopyga*; Walcott, p. 646, pl. 95, figs 1, 1a.
 ?non 1894 *Bathynotus holopygia?*; Peach, p. 671.
 ?non 1907 *Bathynotus holopyga?*; Peach *et al.*, p. 628.
 1910 *Bathynotus holopyga*; Grabau & Shimer, p. 262, fig. 1554.
 1935 *Bathynotus holopyge*; Kobayashi, p. 140.
 1938 *Bathynotus holopygus*; Resser & Howell, p. 230, pl. 12, figs 6, 7.
 1952 *Bathynotus holopygus*; Rasetti, p. 890-891, pl. 1, fig. 5.
 1954 *Bathynotus holopyge*; Kobayashi, p. 25, 26, 32, 39, 40.
 1954 *Bathynotus holopygus*; Shaw (part), p. 1040-1041, USNM localities 319m (=319g) and 25 only (not occurrence at locality SA-C-1).
 1955 *Bathynotus holopygus*; Shaw (part), p. 778 (not pl. 73, fig. 5 = indet. pygidium but not *Bathynotus*).
 1956 *Bathynotus holopyga*; Öpik, p. 44.
 1958 *Bathynotus holopygus*; Shaw, p. 531 (listed in table of occurrences).
 1958 *Bathynotus holopygus*; Lazarenko, pl. 1, fig. 1.
 1959 *Bathynotus holopygus*; Harrington in Harrington *et al.*, p. O64-O65, fig. 48i.
 1959 *Bathynotus holopygus*; Lochman-Balk in Harrington *et al.*, p. O216, fig. 158.1.
 1960 *Bathynotus holopyga*; Balashova & Suvorova in Chernysheva (ed.), p. 128, figs 286a, b.
 1963 *Bathynotus holopyga*; Lu *et al.*, p. 61, pl. 7, fig. 4.
 1965 *Bathynotus holopyge*; Lu *et al.*, p. 93 (mentioned).
 1978 *Bathynotus holopyge*; Yin & Lee, p. 432 (mentioned).
 1981 *Bathynotus holopyge*; Zhang, p. 154 (mentioned).
 1982 *Bathynotus holopyga*; Sun, p. 304 (mentioned).
 ?non 1988 *Bathynotus holopyga?*; Morris, p. 32.
 1988 *Bathynotus holopygus*; Whittington, p. 581-584, 601, 602, pl. 52, figs 1-3, ?4, 5-8, text-fig. 5.
 1990 *Bathynotus sinensis*; Zhao *et al.* (part), p. 46-47, 52, pl. 1, figs 1-4, 6-9, pl. 2, fig. 6, text-fig. 2 only (not pl. 1, fig. 5 = *Bathynotus granulatus*; not pl. 2, fig. 7 = *Bathynotus* sp. indet.).
 1997 *Bathynotus sinensis*; Yuan *et al.*, p. 501 (mentioned).
 1997 *Bathynotus holopygus*; Whittington in Whittington *et al.*, fig. 37.3a-d.
 non 1998a *Bathynotus holopygus*; Palmer, p. 650 (as *Bathynotus*), fig. 4 (in range chart) (= *Bathynotus* sp. or spp. indet.).
 non 1999 *Bathynotus holopygus*; Sundberg *et al.*, p. 104 (= *Bathynotus* sp. or spp. indet.).
 1999 *Bathynotus kueichowensis*; Sundberg *et al.*, p. 107, pl. 1, fig. 1.
 non 2000 *Bathynotus holopygus*; Shergold & Whittington, p. 4-8, figs 2a, b, d, 3 (= *Bathynotus kueichouensis*), fig. 2c (= *Bathynotus* sp. indet.).
 non 2000 *Bathynotus holopygus*; Sundberg & McCollum, p. 604, fig. 2 (in range chart) (= *Bathynotus* sp. or spp. indet.).
 2001 *Bathynotus holopygus*; Yuan *et al.*, pl. 1, fig. 4.
 2002 *Bathynotus holopygus*; Yuan *et al.* (part), p. 86, 232, pl. 7, figs 1-3, 5, 6 only (not pl. 7, fig. 4 = *Bathynotus* sp. indet.).
 2003 *Bathynotus holopygus*; Jell in Jell & Adrain, p. 347.
 2009 *Bathynotus holopygus*; Peng *et al.*, p. 100, 102, 103, 104 (in table 1), figs 1a-d.

Holotype. AMNH 233. This specimen has been illustrated only as line drawings and is now lost (Resser & Howell 1938; Shaw 1955). However, a cast of this specimen exists in the Field Museum, Chicago (FMNH UC13273; also in the Smithsonian Institution [USNM 67610]). A photograph of the plastoholotype is presented here for the first time (Fig. 1A).

Description (specimens > 5mm in sagittal glabellar length). Cranium wide (tr.), subtrapezoidal in

outline; sagittal length 59-73% of transverse distance between distal tips of posterior limbs; distance (tr.) between anterior branches of facial suture at γ 33-40% of distance between distal tips of posterior limbs. Facial suture opisthopian; anterior branches convex abaxially, converging anteriorly to meet at anterior margin; posterior branches short, convex abaxially. Glabella reaches broad anterior border furrow, length 90-95% of cranial length (sag.); broad, trapezoidal, basal glabellar width (tr.) 87-105% of glabellar length (sag.), tapering anteriorly, width (tr.) at distal margins of S2 56-73% of glabellar length (sag.) and 63-83% of basal glabellar width (tr.). LO trapezoidal, exsagittal length at axial furrow 18-25% of glabellar length (sag.); posterior margin convex posteriorly. Sagittal portion of SO straight and transverse; distal portion curves anterolaterally paralleling curvature of posterior margin, shallows in some specimens. L1 subtrapezoidal, exsagittal length at axial furrow 20-25% of glabellar length (sag.). S1 transglabellar; shallow, straight and transverse across sagittal axis; distal portion deepens and trends anterolaterally more strongly than does SO, length (exsag.) of L1 slightly increases distally. L2 arcuate, convex posteriorly; exsagittal length at axial furrow 14-23% of glabellar length (sag.), slightly longer sagittally. S2 deepest abaxially, shallow or absent axially, convex anteriorly either side of sagittal axis with proximal ends located slightly more posteriorly than distal ends; transverse line between intersections of S2 with axial furrows crosses sagittal axis 25-32% of distance from anterior to posterior margin of glabella. S3 very weakly incised, absent axially; trends anterolaterally away from axial furrow, roughly parallel to anterior margin of LA. LA bluntly rounded anteriorly. Anterior cranial border rim-like, sagittal length less than 7% of cranial length (sag.), approximately as wide (tr.) as LA, broadly convex anteriorly and dorsally. Palpebral lobe gently convex dorsally, slightly wider than anterior cranial border, well defined by palpebral furrow which is as broad or slightly broader than palpebral lobe; proximal portion oriented posterolaterally at approximately 60° relative to sagittal axis, curving posteriorly opposite lateral margin of L2 so that distal portion is oriented at approximately 10° relative to sagittal axis; anterior end opposite and close to confluence of S3 and axial furrow, posterior tip opposite SO or lateral margins of LO. Interocular area triangular, tapering anteriorly; width (tr.) opposite posterior tip of palpebral lobe 22-36% of sagittal glabellar length; slightly arched dorsally (tr. and long.; can appear flat on more compacted material). Axial furrow shallow at lateral portion of L3,

L3 more or less confluent with anterior corner of interocular area. Posterior limb of fixigena short (tr.), distal tip barely projects laterally beyond posterior tip of palpebral lobe. Proximal portion of posterior margin of fixigena oriented posterolaterally away from axial furrow at 13-23° relative to transverse line; distal portion flexing slightly anteriorly (and presumably ventrally) at rounded fulcrum. Posterior border well defined by broad border furrow; as wide or slightly wider (exsag.) than anterior border. Small occipital node on posterior portion of LO. External surface of cranium covered with fine to coarse granular ornament except in glabellar, axial, and palpebral furrows (less obvious on internal moulds and on specimens preserved in coarser sediments). Hypostome and presumably fused rostral plate described by Whittington (1988).

Librigena very narrow. Prominent, narrow eye socle directly abuts lateral border furrow or separated from it by extremely narrow (tr.), subtriangular librigenal field. Visual surface unknown. Anterior suture on ventral surface (connective or hypostomal suture) oriented posterolaterally, straight. Lateral border and doublure rounded in cross-section, broadening slightly posteriorly to base of genal spine. Base of genal spines developed opposite lateral margin of LO. Genal spine slender, proximally straight then very slightly curving distally, evenly tapering to pointed tip; length longer than entire trunk, 189-342% of sagittal glabellar length (increasing through ontogeny). Doublure of lateral border and ventral surface of genal spine ornamented with strong terrace ridges.

Thorax of thirteen segments. Axis wide (tr.); axial ring of T1 approximately 60% of total width (tr.) of segment; tapering and proportionally narrowing posteriorly, axial ring of T10 approximately 50% of width (tr.) of segment (excluding pleural spine). Length (sag.) of axial rings approximately 15-24% of axial ring width (tr.). Elongate axial node on each segment. Inner pleural region of T1 oriented posterolaterally relative to transverse axis, tapering distally; margins straight. Inner pleural regions of T2 and T3 progressively more transversely oriented and less tapered distally; those of T4-T10 transverse and parallel-sided. Pleural spines on T1-T3 tiny, thorn-like, sentate, progressively increasing in length posteriorly; pleural spines of T4-T10 progressively increasingly falcate; spine of T10 approximately 5 times longer than length (sag.) of T10 axial ring. T11 macropleural and macrospinous, pleural spine pendant, approximately 10 times longer than length (sag.) of T11 axial ring. Pleurae of T12 and T13 short (tr.), tapering distally, lacking pleural spines;

fused together and to the posterior margin of the pleura of T11; posterior margin of T13 oriented anterolaterally by 10° relative to transverse line. Pleural furrow runs posterolaterally across inner pleural region of T1-T11; steeper-sided anteriorly, barely extending onto pleural spines of segments posterior to T4; anterior pleural band lengthens (exsag.) distally at expense of posterior pleural band. Pleural furrow on T12 and T13 shallow, transverse across inner pleural region. External dorsal surface of thoracic axis and inner pleural regions covered with fine to coarse granular ornament except in furrows; terrace lines on doublure and ventral surfaces of pleural spines.

Pygidium micropygous, sagittal length approximately one-third of cranial length (sag.); roughly semicircular; sagittal length (excluding articulating half ring) just less than half of maximal width (tr.); anterior margin oriented slightly anterolaterally relative to transverse line to fulcrum located approximately three-quarters of distance along margin from axial furrow to anterolateral corner of pygidium; anterior margin distal to fulcrum oriented slightly posteriorly to anterolateral corner of pygidium; maximum pygidial width (tr.) slightly posterior to anterolateral corner, approximately opposite inter-ring furrow. Pygidial axis broad, typically with single axial ring plus undifferentiated terminal piece, separated by straight (tr.) inter-ring furrow; second axial ring is occasionally also expressed (Whittington 1988, pl. 52, fig. 1). Axial furrow shallow anteriorly, represented only by break in slope around lateral and posterior margins of terminal piece. Axial ring subrectangular, width (tr.) at anterior margin of anterior axial ring approximately 50% of distance (tr.) between fulcra, approximately 45% of distance (tr.) between anterolateral corners of pygidium, and approximately 38% of maximal pygidial width (tr.). Terminal piece elongate (sag.) semicircular, smooth; extending to posterior pygidial border. Pleural field smooth except for single, almost effaced, broad interpleural furrow extending from inter-ring furrow, clearest proximally. Broad pygidial border weakly defined by subtle break in slope; maximal width midway around lateral pygidial margin, tapering to anterolateral pygidial corner.

Ontogeny. Specimens examined in the present study that were definitively assigned to this species ranged from 1.8 mm to 16.4 mm in sagittal glabellar length. Several morphological trends are apparent over this sampled portion of ontogeny. Glabellar width generally increases proportionally to sagittal glabellar length (Fig. 7, RMA slopes > 1.0 in Table 4). This proportional

widening is more pronounced in the posterior portion of the glabella (see RMA slopes in Table 4), so that the glabella progressively becomes more anteriorly tapered through ontogeny. The proportional increase in basal glabellar width is matched by an increase in relative width (tr.) of the posterior fixigenae, so that basal glabellar width consistently accounts for 55-61% of the width (tr.) of the posterior cranidium. The proportional length of LO at the axial furrow generally increases slightly from 17% up to approximately 25% of sagittal glabellar length, although with much variation. Genal spine length ranges between 177-233% of sagittal glabellar length on specimens up to 12.5 mm in glabellar length, but increases to over 340% of sagittal glabellar length on larger specimens. The posterior margin of the pygidium bears a medial indentation (the pygidial notch, above) on specimens up to approximately 5 mm in sagittal glabellar length, but this is absent on larger specimens.

Discussion. The analysis presented here demands a more restricted concept of *B. holopygus* compared to that of some previous authors (e.g., Shergold & Whittington 2000). The proportionally long genal spines, extending at least as far as the end of the trunk, in combination with a proportionally wide glabella and a granular ornament, distinguish this species from all congeners. Isolated cranidia of *B. holopygus* are indistinguishable from those of *B. kueichouensis*, leading to some ambiguity in the extent of its geographic and stratigraphic range (discussed below). Only definite occurrences are listed below.

Occurrence. U.S.A.: Vermont. USNM locality 319m (type locality; shale of Noah Parker's Quarry, Parker's Cobble; Fig. 1A, B), and USNM locality 25 (arenaceous dolomite and dolomitic sandstone capping Parker's Cobble, stratigraphically overlying the shale of Parker's Quarry); both occurrences in the Parker Formation (= Parker Shale, Parker Slate) of Franklin County, northwestern Vermont (Shaw 1954).

Shaw (1954, p. 1041; 1955, pl. 73, fig. 5) tentatively identified a fragmentary pygidium from locality SA-C-1 (shale of the Kelly Quarry, Swanton Junction, Vermont) as *B. holopygus*. However, this pygidium (MCZ 5040) does not conform to *Bathynotus* (the pleural field is proportionally much narrower, with the fulcrum located much closer to the axis, and the anterior margin proximal to the fulcrum is oriented slightly posterolaterally rather than anterolaterally away from the axis) and the identification is rejected.

The shale in Parker's Quarry has been estimated to lie between 37 metres and 52 metres

(120 and 170 feet) above the base of the Parker Formation, and probably near the middle of this interval (Shaw 1954; Shaw [1955, p. 778] estimates 46 metres [150 feet]). The arenaceous dolomite and dolomitic sandstone capping Parker's Cobble immediately overlying this shale has been estimated to lie 52 to 64 metres (170 to 210 feet) above the base of the Parker Formation (Shaw 1954; the top of this dolomitic unit had previously been estimated to lie 61 metres [200 feet] above the base of the Parker Formation by Walcott [1886]). All published occurrences of *B. holopygus* from Vermont therefore apparently lie between 37 metres and 64 metres above the base of the Parker Formation, where it co-occurs with the olenelloid trilobites *Mesonacis vermontanus* (Hall, 1859a), *Olenellus thompsoni* (Hall, 1859a), and *O. transitans* (Walcott, 1910), the dorypygids *Kootenia marcoui* (Whitfield, 1884) and *Bonnica capito* (Walcott, 1916), and the eodiscid *Pagetides parkeri* (Walcott, 1886), among other taxa (USNM locality 319m and USNM locality 25 have been used inconsistently by previous workers [discussed by Shaw 1954, p. 1041] and the published faunal lists from these localities should be treated as "inextricably mixed"). Peng *et al.* (2009, p. 103) state that *B. holopygus* is associated with the oryctocephalid trilobite *Lancastria Kobayashi*, 1935 in Vermont (citing Kobayashi 1935). However, neither Resser & Howell (1938) nor Shaw (1954, 1955) list any oryctocephalids in the Parker Formation, and Kobayashi (1935, p. 129) refers to *Lancastria roddyi* (Walcott, 1912) from the Kinzers Formation of Pennsylvania (see also Resser & Howell 1938).

Parker's Quarry has now been entirely quarried away (Shaw 1954, p. 1041), although a small fossil collection from approximately the same horizon at Parker's Cobble was made by Shaw in 1954 (Shaw 1955, p. 804). Scarce but articulated specimens (several in moult configuration, with missing or displaced free cheeks) of *Bathynotus* have recently been collected from the Parker Formation from a site on private land in Vermont (G. Pari, pers. comm. 2001). The site also yields *O. thompsoni* and *M. vermontanus* (G. Pari, pers. comm. 2003).

Dyeran fossils, including the highest occurrence of olenelloids, have been recovered from limestone bioherms at Hall Farm (USNM locality 25a), which Shaw (1954) estimated to lie approximately 137 metres (450 feet) above the base of the Parker Formation and therefore approximately 73 metres above the highest *B. holopygus* occurrence. Shaw (1954, 1958) considered strata lying approximately 177 metres (580 feet) above the base of the Parker Formation (and therefore approximately 113 metres above the highest *B.*

holopygus occurrence) to be probably "Middle Cambrian" (Delamaran of current usage). The Vermont occurrences of *B. holopygus* are therefore late (but not latest) Dyeran in age, but the absence of a high-resolution biostratigraphic zonation for the northern Appalachian region (stemming in part from sparse stratigraphic sampling and in part from a need for modern systematic revision of the faunas) limits more precise age determination. *Kootenia marcoui*, which co-occurs with *B. holopygus* in Vermont, has also been recorded from the carbonates of the lower Henson Gletscher Formation and from the Saeterdal Formation of North Greenland (Blaker & Peel 1997), also of late (but not latest) Dyeran age.

South China. Lower part (*Ovatoryctocara granulata*-*Bathynotus holopygus* Zone) of the Kaili Formation, Yanying village (Yanyin section of Peng *et al.* 2009), northwestern Danzhai County, Guizhou Province (Zhao *et al.* 1990 [described as *B. sinensis*], Yuan *et al.* 2001, 2002; Peng *et al.* 2009).

Bathynotus granulatus Lermontova, 1940 (Figs 1C, 3A, G)

- 1940 *Bathynotus granulatus*; Lermontova, p. 134, pl. 40, figs 2, 2a-e.
 1954 *Bathynotus granulatus*; Kobayashi, p. 25, 26, 32, 40.
 1958 *Bathynotus granulatus*; Lazarenko, p. 18 (mentioned), pl. 1, fig. 2.
 1984 *Bathynotus gaotanensis*; Zhang & Li (part), pl. 1, fig. 3 only (not pl. 1, figs 1, 2, 4 = *Bathynotus* sp. indet.).
 1987 *Bathynotus elongatus*; Zhao *et al.*, p. 43-44, pl. 1, figs 1-6.
 1990 *Bathynotus elongatus*; Zhao *et al.*, p. 49, text-fig. 5, pl. 3, figs 7-9.
 1990 *Bathynotus sinensis*; Zhao *et al.* (part), pl. 1, fig. 5 only.
 1990 *Bathynotus kueichouensis*; Zhao *et al.* (part), pl. 4, fig. 1 only.
 1997 *Bathynotus elongatus*; Yuan *et al.*, p. 501 (mentioned).
 2000 *Bathynotus holopygus*; Shergold & Whittington (part), p. 7 (by inference; *Bathynotus elongatus* = *Bathynotus holopygus*).
 2002 *Bathynotus elongatus*; Yuan *et al.*, p. 86-87, 232, pl. 9, figs 1-3.
 2002 *Bathynotus holopygus*; Yuan *et al.* (part), p. 86 (*Bathynotus granulatus* = *Bathynotus holopygus*).
 2009 *Bathynotus elongatus*; Peng *et al.*, p. 100, 102, 103, 104 (in table 1), figs 1e-h, 2a-d.

Lectotype. The cranidium figured by Lermontova

(1940, pl. 40, fig. 2a; also Lazarenko 1958, pl. 1, fig. 2), designated herein.

Comparative description (specimens > 5 mm in sagittal glabellar length). Cranidium as for *B. holopygus*, with the following differences. Sagittal length of cranidium 66-80% of transverse distance between distal tips of posterior limbs; distance (tr.) between anterior branches of facial suture at γ 36-41% of distance between distal tips of posterior limbs. Glabellar length 90-96% of cranial length (sag.); basal glabellar width (tr.) 69-91% of sagittal glabellar length (increasing through ontogeny), tapering anteriorly, width (tr.) at distal margins of S2 50-61% of glabellar length (sag.) and 61-70% of basal glabellar width (tr.). Exsagittal length of LO at axial furrow 14-25% of glabellar length (sag.). Exsagittal length of L1 at axial furrow 18-27% of glabellar length (sag.). Exsagittal length of L2 at axial furrow 13-20% of glabellar length (sag.), slightly longer sagittally. Transverse line between intersections of S2 with axial furrows crosses sagittal axis 24% to 35% of distance from anterior to posterior margin of glabella. Proximal portion of palpebral lobe oriented posterolaterally at 45-60° relative to sagittal axis, curving posteriorly opposite lateral margin of L2, distal portion is oriented at 5-10° relative to sagittal axis. Width (tr.) of interocular area opposite posterior tip of palpebral lobe 23-36% of sagittal glabellar length. Proximal portion of posterior margin of fixigena oriented posterolaterally away from axial furrow at 11-20° relative to transverse line.

Librigena similar to that of *B. holopygus* except that genal spine is shorter, approximately 132% of sagittal glabellar length on a large specimen (proportionally shorter on smaller specimens; see below), and the genal spine base is more anteriorly located (opposite lateral margins of L1).

Thorax and pygidium indistinguishable from that of *B. holopygus* except that axis is proportionally narrower (transverse width of axis approximately 56-60% of segment width at T1, proportionally tapering posteriorly, transverse width of axis approximately 39-50% of segment width at T10).

Ontogeny. Specimens examined in the present study that were definitively assigned to this species ranged from 2.3 mm to 19 mm in sagittal glabellar length. Several morphological trends are apparent over this sampled portion of ontogeny. The width of the glabella relative to sagittal glabellar length proportionally increases (Fig. 7, RMA slopes > 1.0 in Table 4); basal glabellar width (tr.) proportionally increases from < 60% to > 80% of sagittal glabellar length on specimens

< 2.5 mm up to > 8 mm in sag. glabellar length, and glabellar width across S2 (tr.) proportionally increases from approximately 45% to > 55% of sagittal glabellar length over the same size range. This proportional widening of the axis is also apparent in the posterior region of the thorax and pygidium: the transverse width of the axis of T10 is approximately 39% of the total segment width (excluding pleural spines) on specimens up to 8 mm in sagittal glabellar length but is approximately 50% of the total segment width on the largest articulated specimen (14.5 mm in glabellar length; Fig. 1C).

Cranidia have rarely been found associated with librigenae, and as a result the length of the genal spine is known from very few specimens. Two small specimens from South China with sagittal glabellar lengths 2.6 mm and 3.4 mm have genal spines 65% and 70% of glabellar length, respectively; a much larger specimen (although of unknown actual glabellar length; see Fossil Museum specimen in Appendix 1) has a genal spine 132% as long as its glabella. The posterior margin of the pygidium bears a medial indentation (the pygidial notch, above) on specimens up to approximately 6 mm in sagittal glabellar length (Y. Zhao, pers. comm. January 2009) which is absent on larger specimens. All these trends parallel ontogenetic patterns detected in *B. holopygus* (above).

Discussion. *Bathynotus granulatus* was previously known from two large cranidia, a fragmentary librigena, an articulated posterior portion of the trunk (T7 to T13 plus pygidium), and several thoracic fragments from the Altay-Sayan foldbelt of Siberia (Lermontova 1940; Lazarenko 1958). Yuan *et al.* (2002) considered the species to be synonymous with *B. holopygus*. The analysis presented herein does not support this synonymy, but rather demonstrates conspecificity of *B. granulatus* and *B. elongatus*. The latter species is known from more material, often of high preservational quality (including fully articulated specimens), from South China. Shergold & Whittington (2000) considered *B. elongatus* to be a junior synonym of *B. holopygus*, which is not supported here. *Bathynotus granulatus* (including its junior synonym *B. elongatus*) differs from *B. holopygus* in having a proportionally narrower glabella and thoracic axis, and in having significantly shorter genal spines with posterior tips developed opposite the midlength of the thorax. The proportionally narrow axis also serves to distinguish *B. granulatus* from *B. kueichouensis* and *B. namanensis*, the last of which lacks a granular ornament.

Occurrence. Siberia: Altay-Sayan Foldbelt. "Middle" Cambrian (Amgan?) of the Minusinsk region (Lermontova 1940).

South China. Kaili Formation in Jianghe (formerly Tiajiang) County, eastern Guizhou Province, South China (Yuan *et al.* 2002).

U.S.A.: Nevada. Oak Spring Summit (ICS-10255), uppermost Dyeran; Seven Oaks Spring (ICS-1163), approximately 3.5 metres below base of Delamaran. Both occurrences are in the upper Combined Metals Member, Pioche Formation (Appendix 2).

Bathynotus kueichouensis Lu in Wang, 1964 (Fig. 1D)

1956 *Bathynotus* cf. *holopyga*; Öpik, p. 43-44.

1964 *Bathynotus kueichouensis*; Lu in Wang, p. 27, pl. 2, figs ?2, 3.

1965 *Bathynotus kueichouensis*; Lu *et al.*, p. 93, ?pl. 13, fig. 19.

1975 *Bathynotus* sp. nov.; Öpik, p. 12.

1978 *Bathynotus kueichouensis*; Yin & Lee, p. 432-433, ?pl. 154, fig. 3.

1982 *Bathynotus hubeiensis*; Sun (part), p. 303-304, pl. 2, fig. 5 only (not pl. 1, figs 12-14, pl. 2, figs 4, 6, 7 = *Bathynotus* sp. indet.).

1982 *Bathynotus kueichouensis*; Sun, p. 304 (mentioned).

1982 *Bathynotus hunanensis*; Liu, p. 298, pl. 212, fig. 16, pl. 213, figs 1, 12.

non 1984 *Bathynotus hubeiensis*; Sun, p. 349, pl. 130, figs 7, 8, pl. 133, figs 9, 10 (= *Bathynotus* sp. indet.).

1990 *Bathynotus gaotanensis*; Zhao *et al.* (part), p. 47-48, pl. 2, figs 1-5, pl. 4, fig. 12, text-fig. 3 only (not pl. 1, fig. 10 = *Bathynotus* sp. indet.).

1990 *Bathynotus kueichouensis*; Zhao *et al.* (part), p. 48-49, pl. 3, figs 3-6, 10, text-fig. 4 only (not pl. 4, fig. 1 = *Bathynotus granulatus*).

1990 *Bathynotus* sp. 1; Zhao *et al.* (part), p. 49, pl. 4, figs 3, 4, 6 only (not pl. 4, figs 2, 5 = *Bathynotus* sp. indet.).

1990 *Bathynotus* sp. 2; Zhao *et al.* (part), p. 49-50, pl. 4, fig. 11 only (not pl. 4, figs 7, 8, 9, 10 = *Bathynotus* sp. indet.).

1997 *Bathynotus kueichouensis*; Yuan *et al.* (part), p. 500-501, pl. 2, figs 5, 9 only (not pl. 2, figs 4, 6, 7, 8 = *Bathynotus* sp. indet.).

1997 *Bathynotus hunanensis*; Yuan *et al.*, p. 501 (mentioned).

1999 *Bathynotus gaotanensis*; Yuan *et al.*, pl. 1, fig. 3.

1999 *Bathynotus gaotanensis*; Zhao *et al.*, pl. 1, fig. 6.

2000 *Bathynotus holopygus*; Shergold & Whittington (part), p. 4-8, figs 2a, b, d, 3 only

(not fig. 2c = *Bathynotus* sp. indet.).

2002 *Bathynotus kueichouensis*; Yuan *et al.* (part), p. 87, 232, pl. 7, fig. 7, pl. 8, figs 1-4, pl. 9, figs 4-6 (not pl. 7, fig. 8 = *Bathynotus* sp. indet.).

2007 *Bathynotus kueichouensis*; Wang *et al.* (part), p. 6-8, pl. 1, figs 4-9 only (not pl. 1, figs 1-3 = *Bathynotus* sp. indet.).

2009 *Bathynotus kueichouensis*; Peng *et al.* (part), p. 100, 101-102, 103, 104 (in table 1), figs 1i-l, 2e-f (not figs 2g, h = *Bathynotus* sp. indet.).

Holotype. The large articulated specimen figured by Lu (in Wang 1964, pl. 2, fig. 3), designated herein. This specimen is housed in the Nanjing Institute of Geology and Palaeontology, Chinese Academy of Science (Y. Zhao, J. Yuan and J. Peng, pers. comm., February 2009).

Comparative description (specimens > 5 mm in sagittal glabellar length). Cranium as for *B. holopygus*, with the following differences. Sagittal length of cranium 58-67% of transverse distance between distal tips of posterior limbs; distance (tr.) between anterior branches of facial suture at γ 28-47% of distance between distal tips of posterior limbs. Glabellar length 92-96% of cranial length (sag.); basal glabellar width (tr.) 92-106% of glabellar length (sag.), tapering anteriorly, width (tr.) at distal margins of S2 59-78% of glabellar length (sag.) and 62-75% of basal glabellar width (tr.). Exsagittal length of LO at axial furrow 19-27% of glabellar length (sag.). Exsagittal length of L1 at axial furrow 18-25% of glabellar length (sag.). Exsagittal length of L2 at axial furrow 15-22% of glabellar length (sag.), slightly longer sagittally. Transverse line between intersections of S2 with axial furrows crosses sagittal axis 20-33% of distance from anterior to posterior margin of glabella. Proximal portion of palpebral lobe oriented posterolaterally at approximately 60° relative to sagittal axis, curving posteriorly opposite lateral margin of L2, distal portion is oriented at 5-10° relative to sagittal axis. Width (tr.) of interocular area opposite posterior tip of palpebral lobe 27-34% of sagittal glabellar length. Proximal portion of posterior margin of fixigena oriented posterolaterally away from axial furrow at 6 to 20° relative to transverse line.

Librigena as for *B. holopygus*, with the following differences. Base of genal spines developed opposite lateral margin of L1. Genal spine 84-131% of sagittal glabellar length.

Thorax as for *B. holopygus*, with the following differences. Axis wide (tr.); axial ring of T1 approximately 60% of total width (tr.) of segment; tapering and proportionally narrowing posteriorly, axial ring of T10 approximately 40-50% of width (tr.) of segment (excluding pleural spine). Length

(sag.) of axial rings approximately 17-19% of axial ring width (tr.).

Pygidium as for *B. holopygus*, with the following differences. Outline roughly semicircular with weak medial indentation in posterior margin. Pygidial axis broad, typically with single axial ring plus undifferentiated terminal piece, separated by straight (tr.) inter-ring furrow; second axial ring is occasionally also expressed (Yuan *et al.* 2002, pl. 9, fig. 6).

Ontogeny. Specimens examined in the present study that were definitively assigned to this species ranged from 2.5 mm to 19 mm in sagittal glabellar length. Several morphological trends are apparent over this sampled portion of ontogeny. The width of the glabella relative to sagittal glabellar length proportionally increases (Fig. 7, RMA slopes > 1.0 in Table 4): basal glabellar width (tr.) proportionally increases from approximately 80% to > 90% of sagittal glabellar length, and glabellar width across S2 (tr.) proportionally increases from approximately 60% to approximately 70% of sagittal glabellar length. Genal spine length also typically proportionally increases, from < 80% of sagittal glabellar length on specimens < 4 mm in sagittal glabellar length up to values often > 100% on specimens > 5 mm in sagittal glabellar length. All these trends parallel ontogenetic patterns detected in *B. holopygus* and *B. granulatus* (above). In contrast to *B. holopygus* and *B. granulatus*, however, the posterior margin of the pygidium of *B. kueichouensis* retains a medial indentation (the pygidial notch, above) throughout ontogeny.

Discussion. *Bathynotus kueichouensis* was considered synonymous with *B. holopygus* by Shergold & Whittington (2000), but was considered distinct by Yuan *et al.* (2002; also Wang *et al.* 2007; Peng *et al.* 2009). The present study confirms the distinction between these species. However, only one of the supposed interspecific differences listed by Peng *et al.* (2009, pp. 101-102; above) is actually valid when ontogeny and intraspecific variation are taken into account: the length of the genal spine is consistently shorter throughout ontogeny in *B. kueichouensis* relative to *B. holopygus*. Another difference between *B. kueichouensis* and *B. holopygus* (not mentioned by Peng *et al.* 2009) is that at morphological maturity, *B. kueichouensis* retains a slight sagittal notch in the posterior pygidial margin (Fig. 1D): this notch is lost during ontogeny in *B. holopygus*. *Bathynotus kueichouensis* differs from *B. granulatus* in having a proportionally wider axis, and from *B. namanensis* in possessing a granular ornament.

In contrast to all previous studies, the morphometric analysis presented herein supports assignment of the *Bathynotus* material from Australia to *B. kueichouensis*. This material had previously been considered to represent a new species (Öpik 1956, 1975) or was assigned to *B. holopygus* (Shergold & Whittington 2000 and subsequent authors). Öpik's (1956) supposed differences between this material and *B. holopygus* are not supported: there is no obvious difference in ornament (granulations appear to be present on the external mould figured by Shergold & Whittington [2000, fig. 2a]), and the Australian pygidia (Shergold & Whittington 2000, figs 2b, d) are indistinguishable from those of morphologically mature *B. holopygus* specimens except in perhaps possessing a weak pygidial notch. However, the Australian specimens bear proportionally short genal spines and glabellar dimensions that are indistinguishable from those of *B. kueichouensis*.

Occurrence. China. Lower portion of the Kaili Formation in Jianghe (formerly Tiajiang) and Yuping Counties (eastern Guizhou Province), Cili County (western Hunan Province), Jingshan and Chingyang Counties (Hubei Province), and Guichi County (Anhui Province) in South China, and from Xinjiang in northwest China (Yuan *et al.* 2002; Peng *et al.* 2009).

Australia: Northern Territory. Lower Arthur Creek Formation (Sandover Beds; Ordian or Early Templetonian) at two localities approximately 40 km southeast of Elkedra (Öpik 1956, 1975; Shergold & Whittington 2000).

Bathynotus namanensis Lermontova, 1940 (Fig. 3H)

1940 *Bathynotus namanensis*; Lermontova, p. 134, pl. 40, figs 1, 1a-d.

1951 *Bathynotus namanensis*; Lermontova, p. 97-98, pl. 16, figs 5, 5a-d.

1954 *Bathynotus namanensis*; Kobayashi, p. 26, 41.

1958 *Bathynotus namanensis*; Lazarenko, pl. 1, figs 3-5.

1974 *Bathynotus namanensis*; Ogienko *et al.*, p. 42-43, pl. 7, figs 1-3.

1991 *Bathynotus namanensis*; Astashkin *et al.*, pp. 24, 30.

2001 *Bathynotus namanensis*; Ogienko & Garina, p. 241, figs 7, 8 (in range charts), pl. 12, figs 3-6.

2002 *Bathynotus holopygus*; Yuan *et al.* (part), p. 86 (*B. namanensis* = *B. holopygus*).

Lectotype. Specimen number 153/5156

(Lermontova 1940, pl. 40, fig. 1; Lermontova 1951, pl. 16, fig. 5; Lazarenko 1958, pl. 1, fig. 4; Fig. 3H herein), designated by Ogienko *et al.* (1974, p. 42).

Comparative description (specimens > 5 mm in sagittal glabellar length). Cranidium as for *B. holopygus*, with the following differences. Sagittal length of cranium approximately 63% of transverse distance between distal tips of posterior limbs; distance (tr.) between anterior branches of facial suture at γ 31–40% of distance between distal tips of posterior limbs. Glabellar length 92–93% of cranial length (sag.); basal glabellar width (tr.) 82–92% of glabellar length (sag.), tapering anteriorly, width (tr.) at distal margins of S2 63–72% of glabellar length (sag.) and 69–87% of basal glabellar width (tr.). Exsagittal length of LO at axial furrow 18–22% of glabellar length (sag.). Exsagittal length of L1 at axial furrow 21–27% of glabellar length (sag.). Exsagittal length of L2 at axial furrow 17–25% of glabellar length (sag.), slightly longer sagittally. Transverse line between intersections of S2 with axial furrows crosses sagittal axis 25–28% of distance from anterior to posterior margin of glabella. Proximal portion of palpebral lobe oriented posterolaterally at approximately 60° relative to sagittal axis, curving posteriorly opposite lateral margin of L2, distal portion oriented at 5–10° relative to sagittal axis; anterior end opposite and close to confluence of S3 and axial furrow, posterior tip opposite lateral margins of LO. Width (tr.) of interocular area opposite posterior tip of palpebral lobe 21–39% of sagittal glabellar length. Proximal portion of posterior margin of fixigena oriented posterolaterally away from axial furrow at approximately 12° relative to transverse line. External surface of cranium smooth. Hypostome, librigenae, thorax and pygidium unknown.

Ontogeny. Specimens examined in the present study that were definitively assigned to this species ranged from 4.2 mm to 15 mm in sagittal glabellar length. Mirroring the ontogenetic trends described for other species of *Bathynotus*, the glabella of *B. namanensis* proportionally widens (tr.) through ontogeny: basal glabellar width and width across S2 on the smallest specimen are 76% and 60% of sagittal glabellar length, respectively. This proportional widening is particularly marked in the posterior portion of the glabella: transverse glabellar width across S2 progressively decreases from 78% of basal glabellar width to 69% of basal glabellar width on specimens ranging from 4.2 mm to 8.6 mm in sagittal glabellar length. The smallest specimen

also has a proportionally slightly longer glabella (sagittal length 95% of sagittal cranial length) than all other specimens.

Discussion. Lermontova (1940) stated that *B. namanensis* differed from *B. holopygus* in having a slightly narrower anterior glabella, weaker glabellar furrows (but with a visible S2), and a smooth surface, but the species was synonymised into *B. holopygus* by Yuan *et al.* (2002). Most of these purported differences are equivocal or are not supported by the present study. Glabellar shape is within the range of variation exhibited by *B. holopygus* and *B. kueichouensis*; the difference in the incision of glabellar furrows may be related to preservational mode; and the S2 furrow is also often visible on *B. holopygus* and *B. kueichouensis*. However, the lack of granular ornament on *B. namanensis* is inconsistent with the condition on similarly sized specimens of *B. holopygus* and *B. kueichouensis*. The difference in ornament and the absence of critical information regarding genal spine length and the pygidial outline (i.e., presence or absence of a sagittal notch in the posterior margin) render the purported synonymy of *B. namanensis* and *B. holopygus* tenuous, especially in view of the subtle nature of differences between other species of *Bathynotus* (e.g., *B. holopygus* and *B. kueichouensis*). Based on the material published to date, *B. namanensis* is therefore considered a valid species.

Occurrence. Siberia: Siberian Platform. Base of Zaledeevo Formation near the Angara River (Astashkin *et al.* 1991, p. 24); Chara Formation in the Olekma River region (Astashkin *et al.* 1991, p. 30). Lermontova (1940) first reported the species from limestones in a section along the Namana River, which joins the Lena River close to the Olekma River. Ogienko *et al.* (1974) and Ogienko & Garina (2001) report the species from locality 351 (Angara River) and locality 7104 (Chechuy River, Kirensk region). All occurrences are in the Toyonian (*Namanoia* Zone).

***Bathynotus* sp. or spp. indet.** (Figs 3B–F, 4A–S)

1940 *Bathynotellus yermolaevi*; Lermontova (part), pl. 40, fig. 3b only.

1958 *Bathynotus anabarensis*; Lazarenko, pp. 16–18, pl. 1, figs 6–12.

1969 *Bathynotus fortis*; Semashko, p. 71, 73, pl. 1, figs 3, 4.

1969 *Bathynotus rotundus*; Semashko, p. 71, 73–74, pl. 1, figs 1, 2.

1971 *Bathynotus rotundus*; Semashko in Chernysheva, p. 215–216, pl. 24, figs 1, 2.

- 1979 *Bathynotus* sp.; Ju, p. 304, pl. 1, fig. 1.
 1981 *Bathynotus nanjiangensis*; Zhang, p. 154, pl. 59, fig. 4.
 1982 *Bathynotus hubeiensis*; Sun (part), pl. 1, figs 12-14, pl. 2, figs 4, 6, 7 only.
 1984 *Bathynotus hubeiensis*; Sun, p. 349, pl. 130, figs 7, 8, pl. 133, figs 9, 10.
 1984 *Bathynotus gaotanensis*; Zhang & Li (part), pp. 79, 80, pl. 1, figs 1, 2, 4 only (not pl. 1, fig. 3 = *Bathynotus granulatus*).
 1990 *Bathynotus sinensis*; Zhao *et al.* (part), pl. 2, fig. 7 only.
 1990 *Bathynotus gaotanensis*; Zhao *et al.* (part), pl. 1, fig. 10 only.
 1990 *Bathynotus* sp. 1; Zhao *et al.* (part), pl. 4, figs 2, 5 only.
 1990 *Bathynotus* sp. 2; Zhao *et al.* (part), pl. 4, figs 7, 8, 9, 10 only.
 1991 *Bathynotus anabarensis*; Astashkin *et al.*, p. 84.
 1997 *Bathynotus kueichouensis*; Yuan *et al.* (part), pl. 2, figs 4, 6, 7, 8 only.
 1998a *Bathynotus holopygus*; Palmer, p. 650 (as *Bathynotus*), fig. 4 (in range chart).
 1999 *Bathynotus holopygus*; Sundberg *et al.*, p. 104.
 2000 *Bathynotus holopygus*; Shergold & Whittington (part), fig. 2c only.
 2000 *Bathynotus holopygus*; Sundberg & McCollum, p. 604, fig. 2 (in range chart).
 2001 *Bathynotus angularis*; Ogienko & Garina, p. 242, pl. 33, figs 11-13.
 2001 *Bathynotus* sp.; Ogienko & Garina, p. 242-243, pl. 33, fig. 4.
 2002 *Bathynotus holopygus*; Yuan *et al.* (part), pl. 7, fig. 4 only.
 2002 *Bathynotus kueichouensis*; Yuan *et al.* (part), pl. 7, fig. 8 only.
 2007 *Bathynotus kueichouensis*; Wang *et al.* (part), pl. 1, figs 1-3 only.
 2009 *Bathynotus kueichouensis*; Peng *et al.* (part), figs 2g, h only.

Discussion. The morphometric analysis presented above demonstrates that *B. holopygus* and *B. kueichouensis* can only be distinguished from each other based on librigenal and pygidial morphology. Isolated cranidia cannot be unambiguously assigned to one or other of the species. Similarly, *B. granulatus* or *B. kueichouensis* cannot be distinguished from one another based on isolated librigena (both bear a proportionally short genal spine; above). The species-level identification of many *Bathynotus* specimens is therefore equivocal. Although such indeterminate material is known from all regions, the discussion below focuses only on selected material from Nevada (because these

are new occurrences and offer novel ontogenetic information) and from Siberia (because of the significant impact of the systematic revisions on apparent species diversity there).

U.S.A., Nevada. The first *Bathynotus* specimens recorded from western Laurentia were assigned to *B. holopygus* by Palmer (1998a). Several more specimens have been recovered since the initial finds, but these have received no research attention. The present work finds that the initial identification is questionable: two of the Nevada specimens are here assigned to *B. granulatus* (Figs 1C, 3A, G), and all the other morphologically mature specimens are consistent with assignment to either *B. holopygus* or *B. kueichouensis* and are assigned here to *Bathynotus* sp. or spp. indet. At least two species of *Bathynotus* are therefore present in the uppermost Dyeran of Nevada.

The first documented silicified sclerites of *Bathynotus*, recovered from carbonates in the Hidden Valley and Grassy Spring sections (Appendix 2), provide information regarding the three-dimensional morphology of morphologically immature (presumably meraspid period) cranidia, librigena, and pygidium of the genus. The cranidial convexity in reconstructions of morphologically mature *B. holopygus* (Whittington 1988, text-fig. 5; Shergold & Whittington 2000, fig. 3) is conjectural, being based on compacted specimens. All newly collected morphologically mature specimens of *Bathynotus* from Nevada are also compacted, and shed no new light on the accuracy of the reconstruction of Shergold & Whittington (2000). However, the silicified material of *Bathynotus* sp. indet. described below (Fig. 4) reveals that immature cranidia were strongly vaulted (transversely and longitudinally).

Smallest cranidium (sag. length 1.2 mm; Fig. 4A-D) subpentagonal in outline, approximately as wide (tr.) as long (sag.), relief almost hemispherical (tr. and long.). Posterior margin short (tr.), deflected strongly posterolaterally and ventrally at fulcrum; distance (tr.) between distal tips of the posterior wing approximately 75% of maximal cranidial width. Glabella extends to narrow (sag.) anterior border, relatively narrow (basal width [tr.] approximately 50% of sag. glabellar length), almost parallel-sided posterior to S2, tapers slightly anteriorly to semi-circular anterior margin of LA. Posterior margin of LO strongly convex posteriorly. SO and S1 appear transglabellar; LO tapers distally either side of sagittal axis, occipital node prominent; L1 subrectangular; LO and L1 together comprise approximately 40% of sagittal glabellar length; S2 clear only distally. Palpebral lobe narrow, hugging lateral cranidial margin from just anterior of distal tip of posterior

wings to contact with anterior cranial border; proximal third of palpebral lobe arches strongly upwards, outwards and backwards from border, oriented approximately 60° relative to sagittal axis; medial third of lobe oriented subparallel to sagittal axis; distal third slightly convergent to sagittal axis when followed posteriorly. Interocular area crudely teardrop-shaped, tapering anteriorly, vaulted (tr. and long.), arching strongly ventrally away from axial furrow, dorsal summit of palpebral lobes well below level of axial furrow posterior to LA. Axial furrow does not shallow at lateral margins of L3.

Slightly larger silicified cranidia 1.5 mm and 2.1 mm in sagittal length (Fig. 4E-H and I-L) are similar to the smallest cranium, with the following differences. Cranium progressively proportionally wider (tr.), distance (tr.) between distal tips of posterior wing approximately 80% and 100% of sag. cranial length on these specimens, respectively. Glabella proportionally widens (tr.), particularly posteriorly, basal glabellar width approximately 60% of sag. glabellar length and width at S2 approximately 57% of sagittal glabellar length on largest silicified cranium. Distal portion of palpebral lobe becomes progressively more parallel to sagittal axis (rather than convergent to it posteriorly) over size range of these silicified cranidia. An incomplete cranium of *B. granulatus* preserved in shale (Fig. 3G) with an estimated sagittal cranial length of approximately 2.5 mm is generally similar to the largest silicified cranium, except that the furrows are more pronounced and LO and L1 are more strongly tapered anteriorly. Granular ornament is not evident on any of these small specimens. The silicified cranidia cannot be unequivocally identified to species level.

A single, silicified, isolated librigena (Fig. 4M-O) bears a proportionally short genal spine that dips slightly ventrally relative to the plane of the eye socle. Although the spine tip is broken and glabellar length can only be crudely estimated, the spine would have been only slightly longer than sagittal glabellar length. This is consistent with assignment of the sclerite to either *B. kueichouensis* or *B. granulatus*.

A small silicified pygidium (sagittal length excluding articulating half ring 2.4 mm; Fig. 4P-S) is similar to that described for morphologically mature *B. holopygus* except that a weak sagittal notch is developed in the posterior margin. The morphology of this pygidium is therefore consistent with assignment to immature *B. holopygus*, *B. kueichouensis* or *B. granulatus*. However, it offers insight into the three-dimensional form of the immature pygidium. Anterior margin distal to fulcrum dips ventrally and slightly posteriorly

to anterolateral corner of the pygidium. Pygidial axis strongly vaulted dorsally. Axial furrow shallow anteriorly, represented only by break in slope around lateral and posterior margins of terminal piece. Terminal piece convex dorsally (tr. and sag.), extending to posterior pygidial border. Articulating half ring crescent-shaped, extends full width of axis, maximal length (sag.) almost as long as first axial ring (sag.). Pleural field of low relief, smooth except for single, almost effaced, broad interpleural furrow extending from inter-ring furrow. Interpleural furrow clearest proximally. Broad pygidial border weakly defined by subtle break in slope. Doublure broad (exsag.), with innermost margin below and paralleling break in slope defining pygidial border, tapering anteriorly to apex at anterolateral corner of pygidium distal to fulcrum. Terrace lines on doublure.

Comparison of this silicified material to the larger, morphologically mature material of *Bathynotus* species (above) allows identification of several ontogenetic trends over the earliest sampled portion of ontogeny of species within the genus: 1.) the anterior margin of LA becomes progressively more bluntly rounded; 2.) the distal portion of the palpebral lobe is initially slightly convergent towards the sagittal axis posteriorly, progressively swinging into a posterolaterally divergent orientation; and 3.) the axial furrow is uniformly deep on cranidia up to at least 2.1 mm long (sag.) but shallows at the lateral margins of L3 on cranidia longer than 8 mm (sag.) so that L3 appears confluent with the interocular area. Additional ontogenetic trends are discussed under each species description (above).

Siberia. As many as six species of *Bathynotus* have been named from Siberia. However, the present study suggests that this diversity may be grossly exaggerated. *Bathynotus granulatus* and *B. namanensis* are valid species. Three "species" known from cranidia only (*B. angularis*, *B. rotundus*, and *B. fortis*) are indistinguishable from *B. holopygus* and *B. kueichouensis* given the range of morphological variation (including ontogenetic shape change) within those better-known species. Some Siberian specimens figured as *B. anabarensis* exhibit a glabellar width across S1 and S2 that is almost as narrow (relative to sagittal glabellar length) as that of *B. granulatus* but have a basal glabellar width (proportional to sagittal glabellar length) that is indistinguishable from *B. holopygus* and *B. kueichouensis*, giving the glabella a rather squat, strongly tapered appearance with a more acutely rounded (less blunt) anterior margin of LA. However, these specimens form a cluster subsumed within

the more inclusive “*holopygus*” cluster (on the side closest to the “*granulatus*” cluster) in multivariate morphometric analyses. These four poorly known Siberian taxa cannot be uniquely diagnosed, and are therefore suppressed. Material formerly assigned to these taxa is here treated as *Bathynotus* sp. or spp. indet. (consistent with assignment to either *B. holopygus* and/or *B. kueichouensis*). There is therefore support for the presence of only three species (minimally) of *Bathynotus* in Siberia.

IMPLICATIONS FOR CORRELATION

The revised species-level systematics and corresponding amendments to geographic and stratigraphic ranges of *Bathynotus* species has implications for intercontinental biostratigraphic correlation. Prior to the present work, *B. holopygus* had been reported from eastern Laurentia (Vermont), western Laurentia (Nevada), South China, Australia and the Altay-Sayan Foldbelt of Siberia; all other species were recorded from single palaeocontinents. However, the present work demonstrates that the range of *B. holopygus* may have been overestimated: definitive occurrences are restricted to the upper Dyeran of eastern Laurentia (Vermont) and the upper Duyunian (*Ovatoryctocara granulata-Bathynotus holopygus* Zone) of South China. The current utility of this species for intercontinental biostratigraphic correlation is therefore lessened. Conversely, the distributions of several other *Bathynotus* species were previously underestimated. Reassignment of the Australian material to *B. kueichouensis* expands the range of this species and provides a different species-level tie between the Ordian or Early Templetonian of this continent and the upper Duyunian (*Ovatoryctocara granulata-Bathynotus holopygus* Zone) of South China. *Bathynotus granulatus* is now recognised as the most widespread species within the genus based on definitive occurrences: it provides a species-level tie between the Amgan of the Siberian Altay-Sayan Foldbelt, the uppermost Dyeran (*Nephrolenellus geniculatus* Subzone of the *Nephrolenellus multinodus* Zone) of western Laurentia, and the upper Duyunian (*Ovatoryctocara granulata-Bathynotus holopygus* Zone) of South China.

Bathynotus holopygus does not occur in the same sections as *B. kueichouensis* or *B. granulatus* in South China (Peng *et al.* 2009). Assignment of the South China intervals bearing *B. holopygus* and those bearing *B. kueichouensis* and *B. granulatus* to the same zone is based on correlation utilising other trilobite species. As a result, the distribution of *Bathynotus* species

alone does not permit unequivocal correlation between the *B. holopygus*-bearing strata in eastern Laurentia (Vermont) and South China to other regions of the world.

If individual *Bathynotus* species had short stratigraphic durations (as their ranges in individual sections suggest), and if *B. holopygus* is more or less contemporaneous with *B. kueichouensis* and *B. granulatus* in South China, then the *Ovatoryctocara granulata-Bathynotus holopygus* Zone of South China would correlate with the uppermost Dyeran of eastern and western Laurentia, with the Ordian or early Templetonian of Australia, and with the Amgan of the Siberian Altay-Sayan Foldbelt. Such a correlation is consistent with that shown by Shergold & Cooper (2004, fig. 11.1; although the uppermost Dyeran and Duyunian are depicted as age-equivalent only to the earliest Amgan) and Fletcher (2007, fig. 1), but is inconsistent with that shown by Peng & Babcock (2008, fig. 4.5; where no portion of the Dyeran is depicted as age-equivalent to the Amgan). If the above correlation is accurate, then *B. namanensis*, known only from the Toyonian *Namanoia* Zone of the Siberian Platform, is the oldest known species of *Bathynotus*. It also has the most limited geographic distribution.

It should be reiterated that many *Bathynotus* specimens from around the world (and from western Laurentia and Siberia in particular) cannot be definitively identified to species level: many isolated sclerites are consistent with the diagnoses of more than one species (see above). It is thus entirely possible that *B. kueichouensis* and/or *B. holopygus* also occurs in the uppermost Dyeran of Nevada, or that the ranges of *B. kueichouensis* and/or *B. holopygus* extend into the upper Amgan *Tomagnostus fissus-Paradoxides sacheri* Zone of the Siberian Platform. It is also possible that some or all of these specimens may represent different but currently undiagnosable species. As discussed previously, species discrimination is a hypothesis that is subject to refutation with discovery of new data.

Bathynotus is only one tool for international correlation at the Cambrian Stage 4 to Stage 5 boundary interval. Other taxa inhabiting the same open shelf, outer shelf, shelf edge and slope habitats, such as the oryctocephalids, must be (and are being) brought to bear on the issue. There is currently much discussion regarding the utility of oryctocephalids such as *Oryctocephalus indicus*, *Ovatoryctocara granulata* Chernysheva, 1962, and *Arthricocephalus chauveaui* Bergeron, 1899 in this regard. It is interesting to note that oryctocephalid species-level diagnoses are a matter of heated debate, and a need for assessment of intra- and intercollection

morphological variation in oryctocephalid species has been raised (Fletcher 2007). A study of oryctocephalids employing a species concept and approach analogous to that presented here for *Bathynotus* seems to be warranted. Such an investigation, in combination with that presented here, would create a more defensible systematic framework within which questions pertaining to biogeography, evolution, and biostratigraphic correlation could be more rigorously addressed.

ACKNOWLEDGEMENTS

The first *Bathynotus* specimen from western Laurentia was found by Pat Palmer; others were subsequently collected by Ed Fowler (6 specimens), Linda and Mike McCollum (1), Pete Palmer (4), and Dave Fullmer and the Tom Johnston Team (who together found and generously donated the articulated specimen found at Oak Spring Summit). Giovanni Pari provided information regarding a new site yielding *Bathynotus* in Vermont. Paul Mayer (Field Museum, Chicago) assisted in the loan of specimens. Yuanlong Zhao and Jin Peng kindly provided information and photographs of unfigured material from South China. Adrian Rushton, Paul Shepherd and Mark Dean investigated the whereabouts of the Scottish material. Michael Foote and Leslie Webster were tolerant as I vented about species concepts. Thanks are also extended to John Laurie for his patience in waiting for submission of this manuscript, to Glenn Brock for editing the final typescript, and to Nigel Hughes and Jonathan Adrain for detailed, helpful reviews.

REFERENCES

- ASTASHKIN, V.A., PEGEL, T.V., REPINA, L.N., BELYAEVA, G.V., ESAKOVA, N.V., ROZANOV, A.Y., ZHURAVLEV, A.Y., OSADCHAYA, D.V. & PAKHOMOV, N.N., 1995. The Cambrian System of the Foldbelts of Russia and Mongolia. Correlation Chart and Explanatory Notes. *International Union of Geological Sciences, Publication 32*, 132 p.
- ASTASHKIN, V.A., PEGEL, T.V., SHABANOV, Y.Y., SUKHOV, S.S., SUNDUKOV, V.M., REPINA, L.N., ROZANOV, A.Y. & ZHURAVLEV, A.Y., 1991. The Cambrian System on the Siberian Platform. Correlation Chart and Explanatory Notes. *International Union of Geological Sciences, Publication 27*, 133 p.
- BARRANDE, M.J., 1861. Documents anciens et nouveaux sur la faune primordiale et le Système Taconique en Amérique. *Bulletin de la Société Géologique de France 2, Serie 18*, 203-322.
- BERGERON, J., 1899. Étude de quelques trilobites de Chine. *Bulletin de la Société Géologique de France, Serie 3, 27*, 499-516.
- BLAKER, M.R. & PEEL, J.S., 1997. Lower Cambrian trilobites from North Greenland. *Meddelelser om Grønland, Geoscience 35*, 1-145.
- BRETT, C.E. & ALLISON, P.A., 1998. Paleontological approaches to the environmental interpretation of marine mudrocks. 301-349 in Schieber, J., Zimmerle, W. & Sethi, P.S. (eds.), *Shales and Mudstones. I. Basin Studies, Sedimentology, and Paleontology*. E. Schweizerbart'sche Verlagsbuchhandlung, Stuttgart.
- BRETT, C.E., ALLISON, P.A., TSUJITS, C.J., SOLDANI, D. & MOFFAT, H.A., 2006. Sedimentology, taphonomy, and paleoecology of meter-scale cycles from the Upper Ordovician of Ontario. *Palaaios 21*, 530-547.
- BRETT, C.E. & BAIRD, G.C., 1986. Comparative taphonomy: a key to paleoenvironmental interpretation based on fossil preservation. *Palaaios 1*, 207-227.
- BRETT, C.E. & BAIRD, G.C., 1993. Taphonomic approaches to temporal resolution in stratigraphy: examples from Paleozoic mudrocks. 250-274 in Kidwell, S.M. & Behrensmeier, A.K. (eds.), *Taphonomic approaches to time resolution in fossil assemblages*. Short Courses in Paleontology, 6. Paleontological Society, Knoxville.
- BUDD, A.F. & COATES, A.G., 1992. Nonprogressive evolution in a clade of Cretaceous *Montastraea*-like corals. *Paleobiology 18*, 425-446.
- CHEETHAM, A.H., 1986. Tempo of evolution in a Neogene bryozoan: rates of morphologic change within and across species boundaries. *Paleobiology 12*, 190-202.
- CHERNYSHEVA, N.E., 1960. *Osnovy Paleontologii. Chlenistonogie: Trilobitoobraznye i rakoobraznye*. Akademiia Nauk SSSR, Ministerstvo Geologii i Okhrany Nedr SSSR, Moscow, 515 p.
- CHERNYSHEVA, N.E., 1962. Cambrian trilobites from the Family Oryctocephalidae. *Trudy Nauchno-issledovatel'skogo Instituta Geologii Arktiki Ministerstva Geologii i Ohrani Nedr SSSR 127*, 3-52.
- CHERNYSHEVA, N.E. (ed.), 1971. The Amga Stage of the Altay-Sayan Region. *Trudy SNIIGGIMS 111*, 267 p.
- COWIE, J.W., RUSHTON, A.W.A. & STUBBLEFIELD, C.J., 1972. A correlation of Cambrian rocks in the British Isles. *Geological Society of London, Special Report 2*. 42 p.
- EDDY, J.D. & MCCOLLUM, L.B., 1998. Early Middle Cambrian *Albertella* Biozone trilobites of the Pioche Shale, southeastern Nevada. *Journal of Paleontology 72*, 864-887.
- EDDY, J.D. & MCCOLLUM, L.B., 1999. New name for a Middle Cambrian trilobite and a figure correction. *Journal of Paleontology 73*, 722.
- EMMONS, E., 1860. *Manual of Geology. Second Edition*. A.S. Barnes & Burr, New York, 297 p.
- FLETCHER, T.P., 2007. The base of Cambrian Series 3: the global significance of key oryctocephalid

- trilobite ranges in the Kaili Formation of South China. *Memoirs of the Association of Australasian Palaeontologists* 33, 29-33.
- FOOTE, M. & MILLER, A.I., 2007. *Principles of Paleontology. Third Edition.* W.H. Freeman & Company, New York, 354 p.
- FORTEY, R.A., 1975. Early Ordovician trilobite communities. *Fossils and Strata* 4, 331-352.
- GAINES, R.R. & DROSER, M.L., 2003. Paleoecology of the familiar trilobite *Elrathia kingii*: An early exaerobic zone inhabitant. *Geology* 31, 941-944.
- GEYER, G. & LANDING, E., 2001. Middle Cambrian of Avalonian Massachusetts: Stratigraphy and correlation of the Braintree trilobites. *Journal of Paleontology* 75, 116-135.
- GRABAU, A.W. & SHIMER, H.W., 1910. *North American Index Fossils. Invertebrates. Volume II.* A. G. Seiler and Company, New York, 909 p.
- HALL, B.K. & HALLGRIMSSON, B. (eds.), 2008. *Strickberger's Evolution. Fourth Edition.* Jones & Bartlett Publishers, Sudbury, 760 p.
- HALL, J., 1859a. Trilobites of the shales of the Hudson-River Group. *Twelfth Annual Report of the Regents of the University of the State of New York, on the condition of the State Cabinet of Natural History, and the Historical and Antiquarian Collection connected therewith*, 59-62.
- HALL, J., 1859b. Remarks upon the trilobites of the shales of the Hudson-River Group, with descriptions of some new species of the genus *Olenus*. *Natural History of New York, Paleontology* 3, 525-529.
- HALL, J., 1860. Note upon the trilobites of the shales of the Hudson-River Group in the town of Georgia, Vermont. *Thirteenth Annual Report of the Regents of the University of the State of New York, on the condition of the State Cabinet of Natural History, and the Historical and Antiquarian Collection annexed thereto*, 113-119.
- HALL, J., 1861. Note upon the trilobites of the shales of the Hudson River Group in the town of Georgia, Vermont. 367-372 in Hitchcock, E., Hitchcock, E. Jr., Hager, A.D. & Hitchcock, C.H., *Report on the Geology of Vermont: Descriptive, Theoretical, Economical, and Scenographical. Volume 1.* Claremont Manufacturing Co., Claremont.
- HAMMER, Ø., HARPER, D.A.T. & RYAN, P.D., 2001. PAST: Paleontological statistics software package for education and data analysis. *Palaeontologia Electronica* 4 (1), 1-9.
- HARRINGTON, H.J., HENNINGSMOEN, G., HOWELL, B.F., JAANUSSON, V., LOCHMAN-BALK, C., MOORE, R.C., POULSEN, C., RASETTI, F., RICHTER, E., RICHTER, R., SCHMIDT, H., SDZUY, K., STRUVE, W., STÖRMER, L., STUBBLEFIELD, C.J., TRIPP, R., WELLER, J.M. & WHITTINGTON, H.B., 1959. *Treatise on Invertebrate Paleontology. Part O. Arthropoda 1.* Geological Society of America, New York and University of Kansas Press, Lawrence, 560 p.
- HOPKINS, M.J., & WEBSTER, M., 2009. Ontogeny and geographic variation of a new species of the corynexochine trilobite *Zacanthopsis* (Dyeran, Cambrian). *Journal of Paleontology* 83, 524-547.
- HUGHES, N.C., 1994. Ontogeny, intraspecific variation, and systematics of the Late Cambrian trilobite *Dikelocephalus*. *Smithsonian Contributions to Paleobiology* 79, 89 p.
- HUGHES, N.C., PENG, S. & LUO, H., 2002. *Kunmingaspis* (Trilobita) putatively from the Yunling Collage, and the Cambrian history of the eastern Himalayan syntaxial region. *Journal of Paleontology* 76, 709-717.
- HUPÉ, P., 1953. Classification des Trilobites. *Annales de Paléontologie* 39, 61-168.
- JACKSON, J.B.C. & CHEETHAM, A.H., 1990. Evolutionary significance of morphospecies: A test with cheilostome Bryozoa. *Science* 248, 579-583.
- JACKSON, J.B.C. & CHEETHAM, A.H., 1994. Phylogeny reconstruction and the tempo of speciation in cheilostome Bryozoa. *Paleobiology* 20, 407-423.
- JELL, P.A. & ADRAIN, J.M., 2003. Available generic names for trilobites. *Memoirs of the Queensland Museum* 48, 331-553.
- JU, T.-Y., 1979. Note on the Lower Paleozoic sediments of Suzhou and Hangzhou area (characters of transitional sedimentary region between the Yangtze and the Jiangnan types). *Acta Stratigraphica Sinica* 3, 294-304.
- KOBAYASHI, T., 1935. The Cambro-Ordovician formations and faunas of South Chosen. Palaeontology. Part III. Cambrian faunas of South Chosen with a special study on the Cambrian trilobite genera and families. *Journal of the Faculty of Science, Imperial University of Tokyo. Section II: Geology, Mineralogy, Geography, Seismology* 4 (2), 49-344.
- KOBAYASHI, T., 1954. On the Komaspidae. *Japanese Journal of Geology and Geography* 24, 23-44.
- LANDING, E., 1983. Highgate Gorge: Upper Cambrian and Lower Ordovician continental slope deposition and biostratigraphy, northwestern Vermont. *Journal of Paleontology* 57, 1149-1187.
- LANDING, E. (ed.), 2007. Ediacaran-Ordovician of East Laurentia - S. W. Ford Memorial Volume. 12th International Conference of the Cambrian Chronostratigraphy Working Group. *New York State Museum Bulletin* 510, 94 p.
- LAZARENKO, N.P., 1958. On the discovery of *Bathynotus* in the Cambrian deposits of the northern Siberian Platform. *Sbornik statei po Paleontologii i Biostratigrafii* 8, 15-19.
- LERMONTOVA, E.V., 1940. Class Trilobita. 112-162 in Vologdin, A. (ed.), *Atlas of the leading forms of the fossil faunas of the U.S.S.R. Volume I. Cambrian.* State Editorial Office for Geological Literature, Moscow.
- LERMONTOVA, E.V., 1951. *Lower Cambrian trilobites*

- and brachiopods from eastern Siberia. Vsesoyuznyy Nauchno-Issledovatel'skiy Geologicheskii Institut (VSEGEI), Moscow, 222 p.
- LIEBERMAN, B.S., 2003. A new soft-bodied fauna: the Pioche Formation of Nevada. *Journal of Paleontology* 77, 674-690.
- LIU, Y.R., 1982. Trilobita. 290-346 in *Palaeontological Atlas of Hunan. Geological Memoirs, Series 2, Number 1*. Geological Publishing House, Beijing.
- LU, Y.H., CHANG, W.-T., CHU, C.-L., CHEN, Y.-Y. & HSIANG, L.-W., 1965. *Trilobites of China. (Two Volumes)*. Beijing, Science Publishing Co., 766 p., 135 pls.
- LU, Y.-H., CHIEN, Y.-Y. & ZHU, Z.-L., 1963. Cambrian trilobites. In Chung, S.-Y. (ed.), *Trilobites*. Science Press, Beijing, 186 p., 45 pls.
- MCCOLLUM, L.B. & MCCOLLUM, M.B., 1994. Biostratigraphy of Lower to Middle Cambrian strata in an onshore-offshore transect across the southern Great Basin. *GSA Abstracts with Programs, Cordilleran Section* 26 (2), 71.
- MCCOLLUM, L.B. & SUNDBERG, F.A., 1999. Field Trip Guide: Day 5, Split Mountain and Montezuma Range, Nevada. Stop 9. Biostratigraphy of the traditional Lower-Middle Cambrian boundary interval in the outer shelf Emigrant Formation, Split Mountain East section, Esmeralda County, Nevada. 29-34 in Palmer, A.R. (ed.), *Laurentia 99: V Field Conference of the Cambrian Stage Subdivision Working Group. International Subcommittee on Cambrian Stratigraphy. Utah, Nevada, California, U.S.A., September 12-22, 1999*. Institute of Cambrian Studies, Boulder.
- MCCOLLUM, L.B. & SUNDBERG, F.A., 2007. Cambrian trilobite biozonation of the Laurentian Delamarian Stage in the southern Great Basin, U.S.A.: Implications for global correlations and defining a Series 3 global boundary stratotype. *Memoirs of the Association of Australasian Palaeontologists* 34, 147-156.
- MERRIAM, C.W., 1964. Cambrian rocks of the Pioche Mining District Nevada. *United States Geological Survey Professional Paper* 469, 1-59.
- MIKULIC, D.G., 1990. The arthropod fossil record: Biologic and taphonomic controls on its composition. 1-23 in Mikulic, D.G. (ed.), *Arthropod Paleobiology. Short Courses in Paleontology* 3. Paleontological Society, 316 p.
- MILLER, S.A., 1889. *North American Geology and Palaeontology for the Use of Amateurs, Students, and Scientists*. Cincinnati, 718 p.
- MORRIS, S.F., 1988. *A review of British trilobites, including a synoptic revision of Salter's monograph*. Palaeontographical Society, London, 316 p.
- NIXON, K.C. & WHEELER, Q.D., 1990. An amplification of the phylogenetic species concept. *Cladistics* 6, 211-223.
- OGIENKO, L.V., BYALYI, V.T. & KOLOSITSYNA, G.R., 1974. *Biostratigraphy of the Cambrian and Ordovician deposits of the south Siberian Platform*. Nedra, Moscow, 207 p.
- OGIENKO, L.V. & GARINA, S.Y., 2001. *Stratigraphy and Trilobites in the Cambrian of the Siberian Platform*. Nauchnyi Mir, Moscow, 266 p., 56 pls.
- ÖPIK, A.A., 1956. Cambrian geology of the Northern Territory. *XX Congreso Geológico Internacional XX Sesión, México. El Sistema Cámbrico, su Paleogeografía y el problema de su base. Part II: Australia, América*, 25-54.
- ÖPIK, A.A., 1975. Templetonian and Ordian xystridurid trilobites of Australia. *Bureau of Mineral Resources, Geology and Geophysics, Bulletin* 121, 84 p., 32 pls.
- PALMER, A.R., 1998a. Terminal Early Cambrian extinction of the Olenellina: Documentation from the Pioche Formation, Nevada. *Journal of Paleontology* 72, 650-672.
- PALMER, A.R., 1998b. Why is intercontinental correlation within the Lower Cambrian so difficult? *Revista Espanola de Paleontología, no extr. Homenaje al Prof. Gonzalo Vidal*, 17-21.
- PALMER, A.R., 1998c. A proposed nomenclature for stages and series for the Cambrian of Laurentia. *Canadian Journal of Earth Sciences* 35, 323-328.
- PALMER, A.R. & HALLEY, R.B., 1979. Physical stratigraphy and trilobite biostratigraphy of the Carrara Formation (Lower and Middle Cambrian) in the southern Great Basin. *United States Geological Survey Professional Paper* 1047, 1-131.
- PALMER, A.R. & REPINA, L.N., 1993. Through a glass darkly: Taxonomy, phylogeny, and biostratigraphy of the Olenellina. *University of Kansas Paleontological Contributions, New Series* 3, 1-35.
- PATERSON, J.R., JAGO, J.B., BROCK, G.A. & GEHLING, J.G., 2007. Taphonomy and palaeoecology of the emuellid trilobite *Balcoracania dailyi* (early Cambrian, South Australia). *Palaeogeography, Palaeoclimatology, Palaeoecology* 249, 302-321.
- PEACH, B.N., 1894. Additions to the fauna of the Olenellus-Zone of the Northwest Highlands. *Quarterly Journal of the Geological Society of London* 50, 661-676.
- PEACH, B.N., HORNE, J., GUNN, W., CLOUGH, C.T., & HINXMAN, L.W., 1907. The geological structure of the North-West Highlands of Scotland. *Memoirs of the Geological Survey of Great Britain*, 668 p., 52 pls.
- PENG, S. & BABCOCK, L., 2008. Cambrian Period. 37-46 in Ogg, J.G., Ogg, G. & Gradstein, F.M. (eds.), *The Concise Geologic Time Scale*. Cambridge University Press, Cambridge, 177 p.
- PENG, J., ZHAO, Y., YUAN, J., YAO, L. & YANG, H., 2009. *Bathynotus*: A key trilobite taxon for global stratigraphic boundary correlation between Cambrian Series 2 and Cambrian Series 3. *Progress in Natural Science* 19, 99-105.

- RASETTI, F., 1952. Ventral cephalic sutures in Cambrian trilobites. *American Journal of Science* 250, 885-898.
- REED, F.R.C., 1910. The Cambrian Fossils of Spiti. *Palaeontologia Indica. Geological Survey of India, Series 15, Volume 7, Memoir 1*, 70 p.
- RESSER, C.E. & HOWELL, B.F., 1938. Lower Cambrian *Olenellus* Zone of the Appalachians. *Bulletin of the Geological Society of America* 49, 195-248.
- SEMASHKO, A.K., 1969. New Middle Cambrian trilobites from sandy shale sequences near Juliya Mine (Batenovskiy Ridge). *Isvestiya, Tomsk Ordena Trudovogo Krasnogo Znameni Politekhnikeskogo Instituta Imeni S. M. Kirova* 196, 71-76.
- SHAW, A.B., 1954. Lower and lower Middle Cambrian faunal succession in northwestern Vermont. *Bulletin of the Geological Society of America* 65, 1033-1046.
- SHAW, A.B., 1955. Paleontology of northwestern Vermont. V. The Lower Cambrian fauna. *Journal of Paleontology* 29, 775-805.
- SHAW, A.B., 1958. Stratigraphy and structure of the St. Albans area, northwestern Vermont. *Bulletin of the Geological Society of America* 69, 519-568.
- SHERGOLD, J.H. & COOPER, R.A., 2004. The Cambrian Period. 147-164 in Gradstein, F.M., Ogg, J.G. & Smith, A.G. (eds.), *A Geologic Time Scale 2004*. Cambridge University Press, Cambridge, 589 p.
- SHERGOLD, J.H. & WHITTINGTON, H.B., 2000. The Cambrian trilobite *Bathynotus* (?Redlichioidea) in the Northern Territory, Australia. *Alcheringa* 24, 1-10.
- SMITH, A.B., 1994. *Systematics and the Fossil Record: Documenting Evolutionary Patterns*. Blackwell Science, Oxford, 223 p.
- SOLOVEV, I.A. & GRIKUROV, G.E., 1979. Novye dannye o rasprostraneniі Kembriyskikh trilobitov v khibrakh Ardzhentina i Sheklton. *Antarktika* 18, 54-73.
- SPEYER, S.E., 1987. Comparative taphonomy and palaeoecology of trilobite lagerstätten. *Alcheringa* 11, 205-232.
- SPEYER, S.E. & BRETT, C.E., 1985. Clustered trilobite assemblages in the Middle Devonian Hamilton Group. *Lethaia* 18, 85-103.
- SUN, Z.-H., 1982. Late Lower Cambrian trilobites from southern Dahongshan region, Hubei. *Acta Palaeontologica Sinica* 21, 302-311.
- SUN, Z.-H., 1984. Trilobita. 328-422 in Regional Geological Surveying Team of Hubei (eds.), *The Palaeontological Atlas of Hubei Province*. Hubei Science and Technology Press, Wuhan.
- SUNDBERG, F.A. & MCCOLLUM, L.B., 1997. Oryctocephalids (Corynexochida: Trilobita) of the Lower-Middle Cambrian boundary interval from California and Nevada. *Journal of Paleontology* 71, 1065-1090.
- SUNDBERG, F.A. & MCCOLLUM, L.B., 2000. Ptychopariid trilobites of the Lower-Middle Cambrian boundary interval, Pioche Shale, southeastern Nevada. *Journal of Paleontology* 74, 604-630.
- SUNDBERG, F.A. & MCCOLLUM, L.B., 2002. *Kochiella* Poulsen, 1927, and *Hadrocephalites* new genus (Trilobita: Ptychopariida) from the early Middle Cambrian of western North America. *Journal of Paleontology* 76, 76-94.
- SUNDBERG, F.A. & MCCOLLUM, L.B., 2003a. Trilobites of the lower Middle Cambrian *Poliella denticulata* Biozone (new) of southeastern Nevada. *Journal of Paleontology* 77, 331-359.
- SUNDBERG, F.A. & MCCOLLUM, L.B., 2003b. Early and Mid Cambrian trilobites from the outer-shelf deposits of Nevada and California, USA. *Palaeontology* 46, 945-986.
- SUNDBERG, F.A., YUAN, J.-L., MCCOLLUM, L.B. & ZHAO, Y.-L., 1999. Correlation of the Lower-Middle Cambrian boundary of South China and western United States of America. *Acta Palaeontologica Sinica* 38 (Supplement to part 12), 102-107.
- WALCOTT, C.D., 1886. Second contribution to the studies on the Cambrian faunas of North America. *United States Geological Survey Bulletin* 30, 369 p.
- WALCOTT, C.D., 1890. The fauna of the Lower Cambrian or *Olenellus* Zone. 509-774 in *Tenth Annual Report of the Director, 1888-1889, United States Geological Survey*. United States Geological Survey, Washington.
- WALCOTT, C.D., 1910. Cambrian Geology and Paleontology, Number 6: *Olenellus* and other genera of the Mesonacidae. *Smithsonian Miscellaneous Collections* 53, 231-422.
- WALCOTT, C.D., 1912. Cambrian Geology and Paleontology. II. Number 8. The Sardinian Cambrian genus *Olenopsis* in America. *Smithsonian Miscellaneous Collections* 57(8), 239-249.
- WALCOTT, C.D., 1916. Cambrian Geology and Paleontology. III. Number 5. Cambrian Trilobites. *Smithsonian Miscellaneous Collections* 64(5), 454 p.
- WANG, Y. (ed.), 1964. *Handbook of Index Fossils of South China*. Science Press, Beijing, 173 p., 92 pls.
- WANG, Y.-X., ZHAO, Y.-L., PENG, J. & LI, F.-J., 2007. Study and analysis on extinction of the Lower Cambrian index fossil *Bathynotus*: for instance *Bathynotus kueichouensis* from Kaili Formation, Guizhou. *Journal of Guizhou University of Technology* 37, 6-11.
- WEBSTER, M., 2003. Olenelloid trilobites of the southern Great Basin, U.S.A., and a refinement of uppermost Dyeran biostratigraphy. *Geological Society of America, Abstracts with Programs* 35(6), 166.
- WEBSTER, M., 2005. Intraspecific variability in Early Cambrian olenelloid trilobites: implications for biostratigraphy, regional correlation, and phylogeny. *Acta Micropalaeontologica Sinica* 22 (Supplement),

- 196-197.
- WEBSTER, M., 2007a. Ontogeny and evolution of the Early Cambrian trilobite genus *Nephrolenellus* (Olenelloidea). *Journal of Paleontology* 81, 1168-1193.
- WEBSTER, M., 2007b. *Paranephrolenellus*, a new genus of Early Cambrian olenelloid trilobite. *Memoirs of the Association of Australasian Palaeontologists* 34, 31-59.
- WEBSTER, M., 2009. Ontogeny, systematics, and evolution of the effaced early Cambrian trilobites *Peachella* Walcott, 1910 and *Eopeachella* new genus (Olenelloidea). *Journal of Paleontology* 83, 197-218.
- WEBSTER, M., GAINES, R.R. & HUGHES, N.C., 2008. Microstratigraphy, trilobite biostratigraphy, and depositional environment of the "Lower Cambrian" Ruin Wash Lagerstätte, Pioche Formation, Nevada. *Palaeogeography, Palaeoclimatology, Palaeoecology* 264, 100-122.
- WEBSTER, M. & HUGHES, N.C., 1999. Compaction-related deformation in Cambrian olenelloid trilobites and its implications for fossil morphometry. *Journal of Paleontology* 73, 355-371.
- WEBSTER, M., SADLER, P.M., KOOSER, M.A. & FOWLER, E., 2003. Combining stratigraphic sections and museum collections to increase biostratigraphic resolution. 95-128 in Harries, P.J. (ed.), *High-Resolution Approaches in Stratigraphic Paleontology*. Kluwer Academic Publishers, Dordrecht.
- WHEELER, Q.D. & MEIER, R., 2000. *Species Concepts and Phylogenetic Theory: A Debate*. Columbia University Press, New York, 230 p.
- WHITE, C.A., 1874. Preliminary report upon invertebrate fossils collected by the expeditions of 1871, 1872, and 1873, with descriptions of new species. *U. S. Geographic and Geologic Surveys West of the 100th Meridian Report*, 5-27.
- WHITFIELD, R.P., 1884. Notice on some new species of Primordial fossils in the collections of the museum, and corrections of previously described species. *Bulletin of the American Museum of Natural History* 1 (1881-1886), 139-154.
- WHITTINGTON, H.B., 1988. Hypostomes and ventral cephalic sutures in Cambrian trilobites. *Palaeontology* 31, 577-609.
- WHITTINGTON, H.B., 1998. *Hanburia gloriosa*: rare trilobite from the Middle Cambrian, Stephen Formation, British Columbia, Canada. *Journal of Paleontology* 72, 673-677.
- WHITTINGTON, H.B., CHATTERTON, B.D.E., SPEYER, S.E., FORTEY, R.A., OWENS, R.M., CHANG, W.T., DEAN, W.T., JELL, P.A., LAURIE, J.R., PALMER, A.R., REPINA, L.N., RUSHTON, A.W.A., SHERGOLD, J.H., CLARKSON, E.N.K., WILMOT, N.V. & KELLY, S.R.A., 1997. *Treatise on Invertebrate Paleontology. Part O. Arthropoda 1. Trilobita, Revised. Volume 1: Introduction, Order Agnostida, Order Redlichiida*. Geological Society of America, Boulder and University of Kansas, Lawrence, 530 p.
- YIN, G. & LEE, S., 1978. Trilobita. 385-518, 798-818, pls. 144-171 in *Handbook of Regional Paleontology, Southwest China, Kweichow Province*. Geological Press, Beijing.
- YUAN, J.-L., ZHAO, Y.-L. & GUO, Q.-J., 1999. On the Kaili Formation. *Acta Palaeontologica Sinica* 38 (Supplement to part 12), 22-27.
- YUAN, J.-L., ZHAO, Y.-L. & LI, Y., 2001. Biostratigraphy of oryctocephalid trilobites. *Acta Palaeontologica Sinica* 40 (Supplement), 143-156.
- YUAN, J.-L., ZHAO, Y.-L., LI, Y. & HUANG, Y.-Z., 2002. *Trilobite fauna of the Kaili Formation (uppermost Lower Cambrian-lower Middle Cambrian) from southeastern Guizhou, South China*. National Natural Science Foundation of China, 423 p.
- YUAN, J., ZHAO, Y., WANG, Z., ZHOU, Z. & CHEN, X., 1997. A preliminary study on Lower-Middle Cambrian boundary and trilobite fauna at Balang, Taijiang, Guizhou, South China. *Acta Palaeontologica Sinica* 36, 494-524.
- ZHANG, Q. & LI, C., 1984. The Cambrian trilobites from Gaotan, Guichi County, Anhui Province. *Bulletin of the Nanjing Institute of Geology and Mineral Resources* 5(4), 78-84.
- ZHANG, T.-R., 1981. Trilobita. 134-212 in *Palaeontological Atlas of Northwest China, Volume 1*. Geological Publishing House, Beijing, 332 p., 92 pls.
- ZHAO, Y., GONG, X. & HUANG, Y., 1987. A new species of *Bathynotus* from Lower Cambrian in Taijiang of Guizhou. *Journal of the Guizhou University of Technology* 16, 43-47.
- ZHAO, Y.-L., HUANG, Y.-Z., GONG, X.-Y. & DAI, X.-C., 1990. *Bathynotus* from Kaili Formation (Lower-Middle Cambrian) of Kaili area, Guizhou. *Acta Palaeontologica Sinica* 29, 43-53.
- ZHAO, Y.-L., YUAN, J.-L., ZHU, M.-Y., GUO, Q.-J., ZHOU, Z., YANG, R.-D. & VAN ITEN, H., 1999. The Early Cambrian Taijiang Biota of Taijiang, Guizhou, P.R.C. *Acta Palaeontologica Sinica* 38 (Supplement to part 12), 112-115.
- ZHU, X.-J., HUGHES, N.C. & PENG, S.-C., 2007. On a new species of *Shergoldia* Zhang and Jell, 1987 (Trilobita), the family Tsaniidae and the order Asaphida. *Memoirs of the Association of Australasian Palaeontologists* 34, 243-253.

APPENDIX 1: SPECIMENS

The following table lists all specimens from which data were extracted for the morphometric analysis presented herein. A specimen number was not provided for several specimens figured in the literature. Type specimens of previously named species are indicated. Data were extracted from new and previously published images as indicated in the “Data Source” column. Several specimens have been illustrated more than once in the literature: only the source for the morphometric data used herein is listed. Magnification as quoted in the data source was used for scaling previously published images: any inaccuracies in the precision of the quoted magnifications are assumed to be unbiased. Previous species assignment is listed where appropriate. Locality abbreviations: Sib.: A-S FB, Siberian Altay-Sayan Foldbelt; Sib. Platform, Siberian Platform. The “Fossil Museum specimen” refers to images of an articulated specimen on the Fossil Museum web site (<http://www.fossilmuseum.net/trilobites/Redlichia/Bathynotus-elongatus/Bathynotuselongatus.htm>). Locality details are available, but the specimen carries no identification number nor is a scale bar provided (so morphometric data were not included in the analyses herein). It nevertheless provides useful information regarding the mature morphology of *B. granulatus*.

Specimen Number	Data Source	Previous Species Assignment	Revised Species Assignment	Locality	Sag. Glabellar Length (mm)
gkdo12 (left)	Yuan et al. 2002, pl. 7, fig. 5	holopygus	holopygus	South China	1.8
gkdo12 (right)	Yuan et al. 2002, pl. 7, fig. 5	holopygus	holopygus	South China	2.4
gkdo04	Peng et al. 2009, fig. 1d	holopygus	holopygus	South China	2.64
gkdo10	Yuan et al. 2002, pl. 7, fig. 2	holopygus	holopygus	South China	3.5
gkdo09	Zhao et al. 1990, pl. 1, fig. 3	holopygus	holopygus	South China	4.33
gkdo08	Zhao et al. 1990, pl. 1, fig. 2	holopygus	holopygus	South China	4.67
gkdo02	Zhao et al. 1990, pl. 1, fig. 8	holopygus	holopygus	South China	4.75
gkdo05	Peng et al., 2009, fig. 1b	holopygus	holopygus	South China	5.47
gkdo11	Yuan et al., 2002, pl. 7, fig. 1	holopygus	holopygus	South China	5.5
gkdo07	Zhao et al. 1990, pl. 1, fig. 7	holopygus	holopygus	South China	5.67
YPM 36678	New	holopygus	holopygus	Vermont	12.46
USNM 15409 (255q)	Whittington 1988, pl. 52, fig. 1	holopygus	holopygus	Vermont	13
USNM 15409 (255o)	New	holopygus	holopygus	Vermont	13.25
USNM 15408	Whittington 1988, pl. 52, fig. 4	holopygus	holopygus?	Vermont	14.84
FMNH UC13273 (lectotype)	New	holopygus	holopygus	Vermont	16.42
unknown (lectotype)	Lazarenko 1958, pl. 1, fig. 2	granulatus	granulatus	Sib.: A-S FB	17.42
unknown	Lermontova 1940, pl. 40, fig. 2	granulatus	granulatus	Sib.: A-S FB	19
gtb-29.30-1	Peng et al. 2009, fig. 2d	elongatus	granulatus	South China	2.29
gtb-8-1-23	Peng et al. 2009, fig. 1g	elongatus	granulatus	South China	2.57
gtb-6-1-24	Peng et al. 2009, fig. 1h	elongatus	granulatus	South China	2.71
gtb-30.80-1	Peng et al. 2009, fig. 2c	elongatus	granulatus	South China	2.76
t002	Zhao et al. 1990, pl. 3, fig. 9	elongatus	granulatus	South China	3.43
t033	Zhao et al. 1990, pl. 3, fig. 8	elongatus	granulatus	South China	6.33
gk1088	Unpublished image provided by Jin Peng	elongatus	granulatus	South China	7.82
t010	Zhao et al. 1990, pl. 4, fig. 1	kueichouensis	granulatus	South China	8.17
gkdo03	Zhao et al. 1990, pl. 1, fig. 5	holopygus	granulatus	South China	8.79
gkt001 (holotype)	Yuan et al. 2002, pl. 9, fig. 1	elongatus	granulatus	South China	8.83
gk1089	Yuan et al. 2002, pl. 9, fig. 3	elongatus	granulatus	South China	10.75
gtb-38.50-2	Peng et al. 2009, fig. 2a	elongatus	granulatus	South China	14.9
Fossil Museum specimen	Fossil Museum web site	N/A	granulatus	South China	.
FMNH PE58132	New	N/A	granulatus	Nevada	2.42
FMNH PE58120	New	N/A	granulatus	Nevada	14.48
gtb-8-1-47	Peng et al. 2009, fig. 11	kueichouensis	kueichouensis	South China	2.46
Peng collection (2)	Unpublished image provided by Jin Peng	N/A	kueichouensis	South China	2.58
t015	Zhao et al. 1990, pl. 4, fig. 3	kueichouensis	kueichouensis	South China	4
gkto24	Yuan et al. 2002, pl. 8, fig. 4	kueichouensis	kueichouensis	South China	5.78
gk4402	Yuan et al. 2002, pl. 8, fig. 1	kueichouensis	kueichouensis	South China	6.88
Peng collection (4)	Unpublished image provided by Jin Peng	N/A	kueichouensis	South China	7.13
FMNH PE58139	New	N/A	kueichouensis	South China	11
t022	Zhao et al. 1990, pl. 2, fig. 5	kueichouensis	kueichouensis	South China	12
Peng collection (7)	Unpublished image provided by Jin Peng	N/A	kueichouensis	South China	12.89
gk1091	Yuan et al. 2002, pl. 9, fig. 6	kueichouensis	kueichouensis	South China	16.67
gk1090	Yuan et al. 2002, pl. 9, fig. 5	kueichouensis	kueichouensis	South China	19.23
gkto23	Yuan et al. 2002, pl. 8, fig. 2	kueichouensis	kueichouensis	South China	.
CPC34703	Shergold & Whittington 2000, fig. 2b	holopygus	kueichouensis	Australia	6.12
CPC34704	Shergold & Whittington 2000, fig. 2a	holopygus	kueichouensis	Australia	6.17
418-g-3	Ogienko & Garina 2001, pl. 12, fig. 6	namanensis	namanensis	Sib. Platform	4.2
138/1969	Ogienko et al. 1974, pl. 7, fig. 1	namanensis	namanensis	Sib. Platform	5
35/1969	Ogienko et al. 1974, pl. 7, fig. 2	namanensis	namanensis	Sib. Platform	5.6
139/1969	Ogienko et al. 1974, pl. 7, fig. 3	namanensis	namanensis	Sib. Platform	6.67
153/5156 (lectotype)	New	namanensis	namanensis	Sib. Platform	8.62

Specimen Number	Data Source	Previous Species Assignment	Revised Species Assignment	Locality	Sag. Glabellar Length (mm)
155/5156	Lazarenko 1958, pl. 1, fig. 3	namanensis	namanensis	Sib. Platform	14.83
gk1084	Yuan et al. 2002, pl. 7, fig. 4	holopygus	sp. indet.	South China	4.17
gtb-29.20-1	Peng et al., 2009, fig. 2g	kueichouensis	sp. indet.	South China	2.61
gtb-30.80-3	Peng et al., 2009, fig. 2h	kueichouensis	sp. indet.	South China	2.76
t029	Zhao et al. 1990, pl. 4, fig. 9	kueichouensis	sp. indet.	South China	3.5
NIGP 127379	Yuan et al. 1997, pl. 2, fig. 7	kueichouensis	sp. indet.	South China	3.56
NIGP 127376	Yuan et al. 1997, pl. 2, fig. 4	kueichouensis	sp. indet.	South China	3.83
t017	Zhao et al. 1990, pl. 4, fig. 5	kueichouensis	sp. indet.	South China	4.5
t028	Zhao et al. 1990, pl. 4, fig. 8	kueichouensis	sp. indet.	South China	5.71
t027	Zhao et al. 1990, pl. 4, fig. 7	kueichouensis	sp. indet.	South China	6
gk1086	Yuan et al. 2002, pl. 7, fig. 8	kueichouensis	sp. indet.	South China	6
NIGP 127378	Yuan et al. 1997, pl. 2, fig. 6	kueichouensis	sp. indet.	South China	6.25
t032	Zhao et al. 1990, pl. 1, fig. 10	kueichouensis	sp. indet.	South China	15.11
unknown	Lazarenko 1958, pl. 1, fig. 11	anabarensis	sp. indet.	Sib. Platform	3.11
unknown	Lazarenko 1958, pl. 1, fig. 7	anabarensis	sp. indet.	Sib. Platform	3.26
unknown	Lazarenko 1958, pl. 1, fig. 6	anabarensis	sp. indet.	Sib. Platform	3.27
unknown	Lazarenko 1958, pl. 1, fig. 8	anabarensis	sp. indet.	Sib. Platform	3.59
unknown	Lazarenko 1958, pl. 1, fig. 12	anabarensis	sp. indet.	Sib. Platform	3.76
unknown	Lazarenko, 1958, pl. 1, fig. 9	anabarensis	sp. indet.	Sib. Platform	4.62
unknown	Lazarenko 1958, pl. 1, fig. 10	anabarensis	sp. indet.	Sib. Platform	4.64
442-614	Ogienko & Garina 2001, pl. 33, fig. 13	angularis	sp. indet.	Sib. Platform	2
437-613 (holotype)	Ogienko & Garina 2001, pl. 33, fig. 11	angularis	sp. indet.	Sib. Platform	2.86
437-612	Ogienko & Garina 2001, pl. 33, fig. 12	angularis	sp. indet.	Sib. Platform	4
4734/5 (holotype)	Semashko 1969, pl. 1, fig. 3	fortis	sp. indet.	Sib.: A-S FB	5.2
4734 (holotype)	Chernysheva 1972, pl. 24, fig. 1	rotundus	sp. indet.	Sib.: A-S FB	3
4734/2	Chernysheva 1972, pl. 24, fig. 2	rotundus	sp. indet.	Sib.: A-S FB	3.13
FMNH PE58136	New	N/A	sp. indet.	Nevada	1.1
FMNH PE58137	New	N/A	sp. indet.	Nevada	1.44
FMNH PE58138	New	N/A	sp. indet.	Nevada	2.03
ICS-1163.3	New	N/A	sp. indet.	Nevada	6.78
ICS-1163.4	New	N/A	sp. indet.	Nevada	7.12
FMNH PE58128	New	N/A	sp. indet.	Nevada	7.55
FMNH PE58131	New	N/A	sp. indet.	Nevada	7.78
FMNH PE58126	New	N/A	sp. indet.	Nevada	9.47
FMNH PE58127	New	N/A	sp. indet.	Nevada	10.69
FMNH PE58135	New	N/A	sp. indet.	Nevada	.
Peng collection (8)	Unpublished image provided by Jin Peng	N/A	sp. indet.	South China	2.09
Peng collection (3)	Unpublished image provided by Jin Peng	N/A	sp. indet.	South China	3.25
Peng collection (1)	Unpublished image provided by Jin Peng	N/A	sp. indet.	South China	3.51
Peng collection (6)	Unpublished image provided by Jin Peng	N/A	sp. indet.	South China	3.91
Peng collection (9)	Unpublished image provided by Jin Peng	N/A	sp. indet.	South China	4.66
Peng collection (10)	Unpublished image provided by Jin Peng	N/A	sp. indet.	South China	5.56
Peng collection (5)	Unpublished image provided by Jin Peng	N/A	sp. indet.	South China	6.59
Peng collection (11)	Unpublished image provided by Jin Peng	N/A	sp. indet.	South China	6.89
Peng collection (12)	Unpublished image provided by Jin Peng	N/A	sp. indet.	South China	7.28

APPENDIX 2: SECTIONS

The location of each of the measured sections (Figs 2, 9-12) is detailed below. Dyeran and Delamaran ptychoparioid and corynexochid trilobites from many of these localities were described by Eddy & McCollum (1998, 1999), Sundberg & McCollum (2000, 2002, 2003a), and Hopkins & Webster (2009); *Nephrolenellus* occurrences were noted by Webster (2007a). The new species of *Olenellus* will be described elsewhere (Webster, in preparation).

Oak Spring Summit section, Delamar Mountains (Fig. 9)

37° 37.198' N, 114° 43.170' W. Section measured and collected by A. R. Palmer (1991, 1992, 1995, 1999, 2000) and by MW (1997, 2000, 2001, 2005). This is the stratotype section for the Dyeran-Delamaran boundary (Palmer 1998c), and the uppermost Delamar Member through Comet Shale Member are well exposed. Following the lithostratigraphic revisions of Sundberg & McCollum (2000), the top of the Combined Metals Member is now defined as the base of the ribbon limestone containing the ptychoparioid "*Eokochaspis*" *nodosa* (coinciding with the Dyeran-Delamaran boundary), which occurs 29.88 metres above the base of the Combined Metals Member at Oak Spring Summit. The lowermost 16.60 metres of the Combined Metals Member form

a series of prominent cliffs and ledges; the upper 13.28 metres are comprised of more recessive strata (5.0 metres of rubbly-weathering, nodular carbonate, overlain by 8.28 metres of shale). The thickness of the more recessive portion of the member at Oak Spring Summit has previously been quoted as almost 11 metres (Palmer 1998a) and as approximately 12.5 metres (Palmer 1998c), in close agreement with the value obtained in the present study. *Bathynotus* sp. indet. occurs in collection ICS-1024 (shale from the heavily quarried area in the upper 3.0 metres of the Combined Metals Member). An articulated specimen of *B. granulatus* was recovered from collection ICS-10255 (shale from the uppermost Combined Metals Member at a site approximately 600 metres SSE of the main section, at 37° 36.872' N, 114° 42.964' W).

Hidden Valley section, Burnt Springs Range (Fig. 10) 37° 36.625' N, 114° 45.592' W. Section measured and collected by A. R. Palmer (1995-1997, 1999), by MW (1997, 2001), and by E. Fowler. A well exposed and fossiliferous section of the upper Combined Metals Member and basal Comet Shale Member. *Bathynotus* sp. indet. occurs in collections ICS-1186 (shale 4.9 metres below the base of the Delamaran), ICS-1173 (carbonate bed 2.06 metres to 1.80 metres below the base of the Delamaran, bearing a rich silicified fauna; see also Webster & Hughes [1999]; Webster

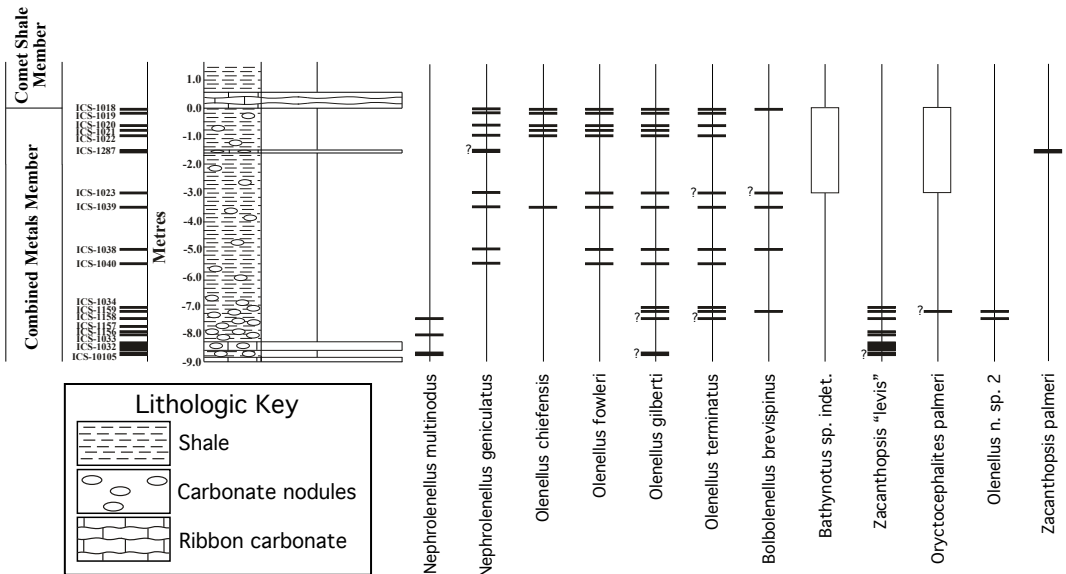


Fig. 9. Lithologic log and biostratigraphic range chart for non-ptychoparioid trilobites in the upper Combined Metals Member of the Pioche Formation (latest Dyeran, traditional "Lower Cambrian" of Laurentia) at the Oak Spring Summit section, Delamar Mountains. Metre scale indicates stratigraphic distance below base of ribbon limestone marking base of Delamaran (traditional "Middle Cambrian" of Laurentia). Black bars to left of metre scale indicate provenance of stratigraphically constrained fossil collections housed in the ICS, open boxes indicate less well constrained fossil collections in the ICS. A question mark next to a black bar indicates a tentative identification. Except for *Bathynotus*, stratigraphic occurrences of specimens identifiable only to superspecific taxonomic level are not shown.

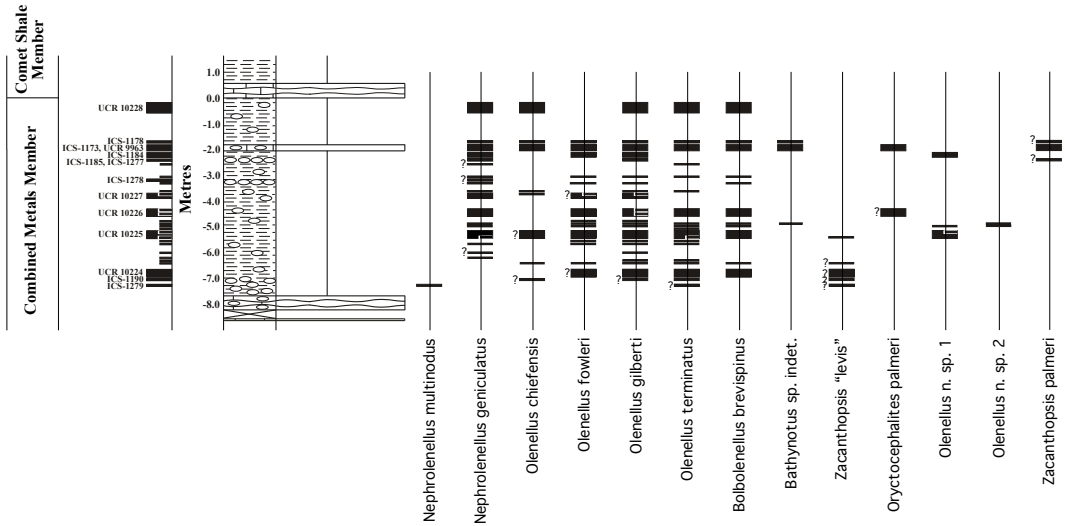


Fig. 10. Lithologic log and biostratigraphic range chart for non-ptychoparioid trilobites in the upper Combined Metals Member of the Pioche Formation (latest Dyeran, traditional “Lower Cambrian” of Laurentia) at the Hidden Valley section, Burnt Springs Range. Layout and lithologic symbols as for Fig. 9. Stratigraphically constrained fossil collections indicated by unlabeled small black bars to left of metre scale are contained with broader collection ICS-1186.

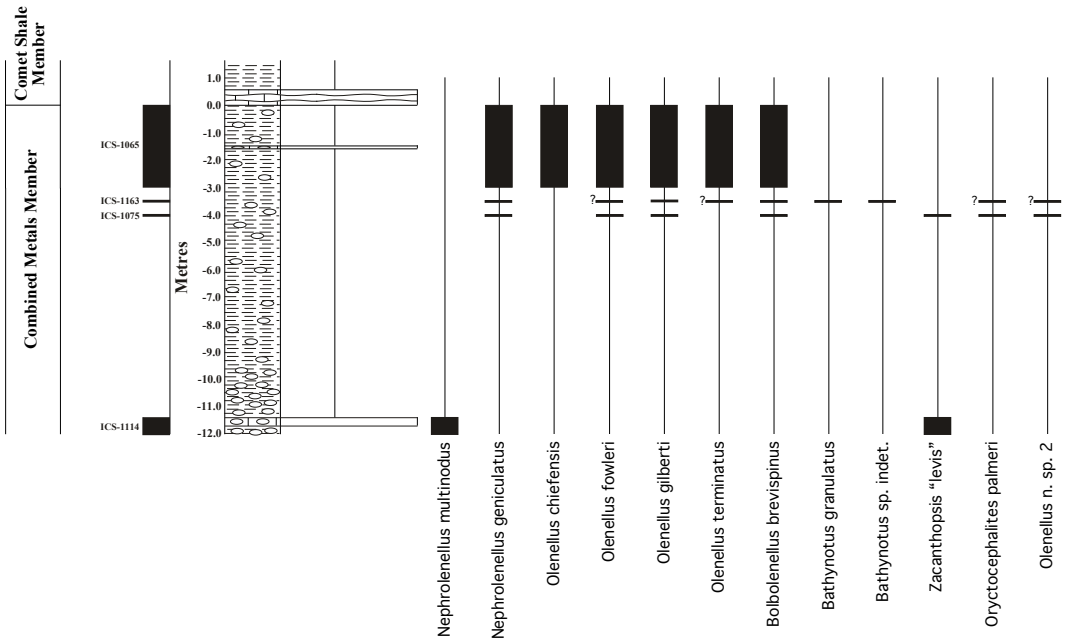


Fig. 11. Lithologic log and biostratigraphic range chart for non-ptychoparioid trilobites in the upper Combined Metals Member of the Pioche Formation (latest Dyeran, traditional “Lower Cambrian” of Laurentia) at the Seven Oaks Spring section, Burnt Springs Range. Layout and lithologic symbols as for Fig. 9.

[2007a]; Hopkins & Webster [2009]), and ICS-1178 (shale approximately 1.7 metres below the base of the Delamaran).

Seven Oaks Spring section, Burnt Springs Range (Fig. 11)

Approximate coordinates 37° 35.913' N, 114° 45.173' W. Section collected by A. R. Palmer (1993) and by E.

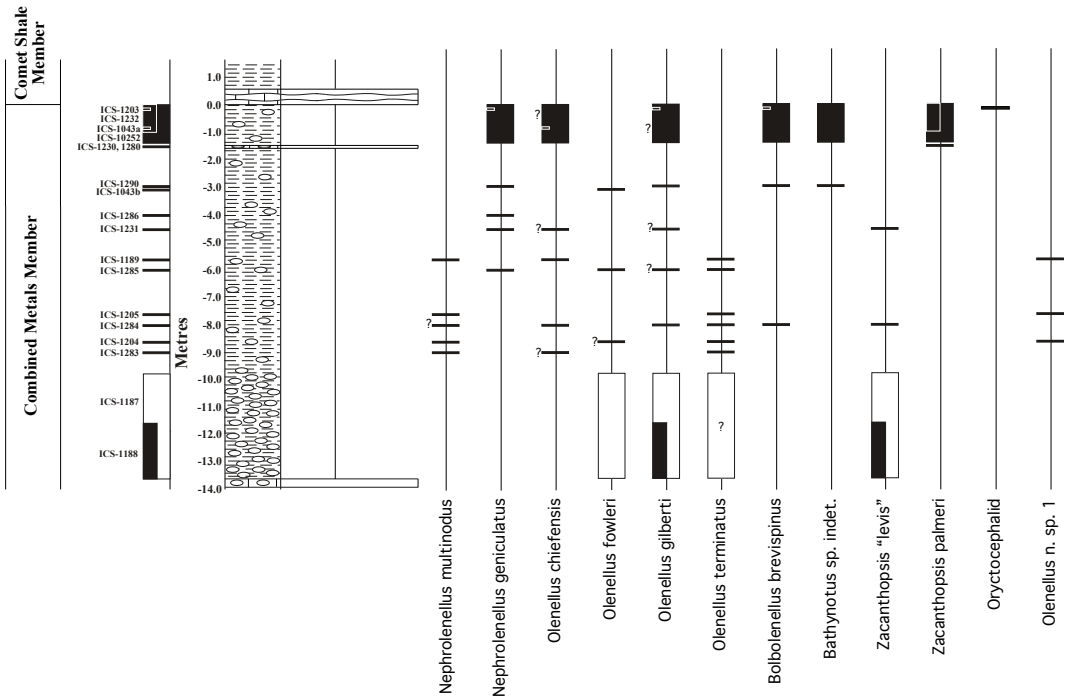


Fig. 12. Lithologic log and biostratigraphic range chart for non-ptychoparioid trilobites in the upper Combined Metals Member of the Pioche Formation (latest Dyeran, traditional “Lower Cambrian” of Laurentia) at the Grassy Spring section, Delamar Mountains. Layout and lithologic symbols as for Fig. 9.

Fowler (1995). See also Palmer (1998a). *Bathynotus granulatus* and *Bathynotus* sp. indet. occur in collection ICS-1163 (shale approximately 3.5 metres below the base of the Delamaran; material found by E. Fowler may have been collected slightly below this).

Grassy Spring section, Delamar Mountains (Fig. 12) 37° 31.244' N, 114° 47.508' W. Section measured and collected by A. R. Palmer (1992, 1996-1999; see

Palmer [1998a]) and by MW (1997). A reasonably well exposed and fossiliferous section of the upper Combined Metals Member and basal Comet Shale Member. *Bathynotus* sp. indet. occurs in collections ICS-1290 (silty carbonate nodules from 3 metres below the base of the Delamaran, bearing a sparse silicified fauna) and ICS-10252 (carbonate nodules from 1.5 metres to 0.0 metres below the base of the Delamaran, bearing a silicified fauna).